Proceedings of the International Conference on Creationism

Volume 9
Print Reference: 363-386

Article 13

2023

The Role of Large Tsunamis in the Formation of the Flood Sediment Record

John Baumgardner
Liberty University

Evan Navarro
Delta Star, Inc.

Baumgardner, J., and E. Navarro. 2023. The role of large tsunamis in the formation of the Flood sediment record. In J.H. Whitmore (editor), *Proceedings of the Ninth International Conference on Creationism*, pp. 363-386. Cedarville, Ohio: Cedarville University International Conference on Creationism.

THE ROLE OF LARGE TSUNAMIS IN THE FORMATION OF THE FLOOD SEDIMENT RECORD

John R. Baumgardner, School of Engineering, Liberty University, Lynchburg, Virginia, jrbaumgardner@liberty.edu
Evan Navarro, Delta Star, Inc., en8hb@virginia.edu

ABSTRACT

A major challenge for Flood geology is providing a credible explanation for how the staggering volume of fossil-bearing sediment was eroded, transported, and deposited in orderly patterns on the surface of the normally high-standing continents in only a few months' time. This paper builds upon the numerical modeling work reported at the 2018 ICC (Baumgardner 2018b) utilizing a code named MABBUL which showed that repetitive giant tsunamis generated by catastrophic plate tectonics (CPT) during the Genesis Flood can plausibly account for the Flood sediment record. That modeling demonstrated that, with reasonable parameter choices, tsunami-driven cavitation erosion during the Flood itself, mostly along the continent margins, can produce most of the sediment in today's fossil-bearing record. The modeling showed further that tsunami-driven pulses of turbulent water can transport this sediment vast distances across the continental surfaces and that these hydrological processes generate sequences of laterally extensive layers often separated by erosional unconformities. That model included a realistic time history of the continental blocks to explore the influence of continental motions on the overall patterns of erosion and sedimentation. It also included an initial continental topography, with low elevations along the coasts and higher elevations inland. Astonishingly, but not mentioned in that paper, the large-scale sediment distribution pattern generated in that model matched remarkably well the large-scale features of the actual sediment distribution of today's world.

This paper includes a more accurate continent motion history and runs at double the horizontal spatial resolution with grid points spaced only 60 km apart. It makes a beginning attempt to model the processes responsible for the megasequence structure of the Flood sediment record. It assumes that the erosional unconformities between the megasequences were caused by abrupt drops in global sea level, which in turn are assumed to be expressions of episodes of rapid cooling of the ocean lithosphere. The revised version of MABBUL, in addition to offering new insight concerning the megasequences, continues to yield a large-scale sediment distribution pattern that matches the observed pattern remarkably well.

KEYWORDS

Genesis Flood, Flood sediment record, large tsunamis, catastrophic plate tectonics, turbulent sediment transport, open channel flow, cavitation erosion, megasequences

I. INTRODUCTION

Panoramic views of the sediment layers that blanket the continents as displayed in the Grand Canyon, for example, reveal a radical contrast between erosion and sedimentation regimes of the past and what prevails today. Fig. 1, a photo from the south rim of the Grand Canyon, reveals a layer-cake style of sedimentation with hundreds of distinct individual layers with vast lateral extent, almost uniform thickness, and boundaries between successive layers that are nearly smooth. These features are not atypical but typical of the global Phanerozoic sedimentary record as documented by numerous surface exposures and by tens of thousands of well logs from wells drilled into the subsurface for the purpose of petroleum exploration and production. By contrast, the higher elevation portions of the continental surface today are strongly sculpted by erosional processes and dissected by erosional channeling. Sedimentation generally is localized, mostly to stream and river channels and deltas. Given that erosional features are so prevalent across the continental surfaces today, why are they so infrequent on the strata boundaries in the underlying sediment record?

Moreover, cross-bedding is common within individual layers throughout the record. Cross-bedding in a water-deposited sediment layer requires relatively high water speeds that produce migrating dunes, with sediment deposition on the front side of the dunes where the local water velocity becomes small because of the eddies that form there. The fact that these cross-bedded layers commonly display large horizontal extent, up to hundreds of km, transverse to the flow direction means that the water flow is sheetlike in character. There is no analogous process occurring on the continents today. A crucial question begging for an answer is what sort of process could conceivably drive and sustain relatively uniform high-speed water flow over such vast areas on the continental surface and do so repeatedly to account for many cross-bedded layers throughout the vertical column?

Another point of contrast between geological processes occurring today relative to those of the past pertains to the preservation of distinct sedimentary layers. Because burrowing organisms are so

Figure 1. Photo from the south rim of the Grand Canyon, Arizona, USA.

active and prolific, any layering that may occur in today's world in most cases is quickly obliterated by these organisms. However, the presence of the sort of well-defined layers so evident from bottom to top of the Phanerozoic record is in stark contrast with what we observe in today's sedimentary environments.

Another prominent attribute of these sediment layers is their fossil content. Fossilization generally requires that an organism be completely and rapidly buried; otherwise, the organism when it dies will soon lose its identifying features because of scavengers and micro-organisms. Hence, fossils are a reliable indicator of an extraordinary rate of sedimentation. The fact that fossils are so common throughout the Phanerozoic sediment record argues that most of that record must be the product of high-rate sedimentary processes.

Yet another feature of the fossil record argues that the total time span for the formation of this record has been no more than a few thousands of years. This evidence is the excellent state of preservation of soft tissue in fossils across the record. Examples include flexible blood vessels containing red blood cells in a femur from Tyrannosaurus rex (Schweitzer et al. 2005), flexible bone tissue, delicate bone cells known as osteocytes, and red blood cells from a Triceratops horridus horn (Armitage and Anderson 2013), and collagen and red and white blood cells from an ichthyosaur vertebra (Plet et al. 2017).

Such striking contrasts between the geological processes operating today and those responsible for the fossil-bearing sediments averaging some 1,800 m in thickness that blanket the earth's continents pose a profound challenge to a premise foundational to modern geological understanding. This premise, adopted in the shadow of the Enlightenment some 200 years ago, is that present-day geological processes, operating at approximately presently observed rates, explain the earth's rock record with a high degree of fidelity since early in earth history. This premise is generally referred to as uniformitarianism. Expressed more briefly, it is the claim that "the present is the key to the past" in terms of geological processes. However, the glaring points of conflict just outlined between past processes and rates and those of the present are sufficiently serious and also so well-supported by observation as to render that premise false and rationally indefensible. The implication is that the field of geology veered into the weeds 200 years ago and has since been lost there ever since.

But if uniformitarianism is so profoundly deficient, is there a rational alternative? Indeed there is, namely, the view held by most people in the Western world, even among the well-educated, prior to the late 1700s. It is the understanding that the earth's fossil-bearing geological record is a consequence of the global cataclysm described in chapters 6-8 of Genesis. This is the strong conviction of this paper's authors.

II. BACKGROUND

Just what might a rational defense of the Genesis Flood, within the backdrop of 21st century science, look like? One essential feature is a zeal to examine the full spectrum of observational evidence, including that summarized in the previous section. Another is a zeal to apply the full spectrum of well-tested physical laws to gain insight into the physical processes involved, along with a diligence to obtain quantitative estimates of the process rates as constrained by the time scale provided in the Genesis text. Another is to deal carefully with the tension between the reality that there is a natural order which God Himself established and the fact that God is fully able to overrule that natural order when He so chooses. On this it is to be noted that 2 Peter 3:3-6 implies that God did overrule the natural order in some significant manner during the Flood.

As an example of this strategy, let us address one of the more challenging features of the sediment record to explain. This is the vast lateral extent of a significant fraction of the layers as highlighted in the discussion of Fig. 1. It is not uncommon for layers to extend for 1,000 km in one direction and for hundreds of km in the perpendicular direction, often with little variation in layer thickness, sediment grain size, or composition. One question that naturally arises is what sort of water process could suspend, transport, and deposit such a huge volume so uniformly over such a vast area?

A. Quantifying the sediment transport and deposition process

To deal with that topic in a qualitative way it is helpful to have some estimate for the average rate of sediment deposition over the continental surface during the cataclysm. The average thickness of the fossil-bearing sediment sequence blanketing the continents today is estimated to be between 1,800 m and 2,000 m (Prothero and Schwab 2004; Olson et al. 2016; Baumgardner 2018b). Assuming most of the Flood's primary deposition occurred within the interval of 150 days during which "the water prevailed on the earth" (Genesis 7:24), one can divide the lower estimate of 1,800 m by 150 days to obtain an average deposition rate of 12 m/day (equivalent to 39.4 ft/day, 0.5 m/hr, or 1.4×10^{-4} m/s). If most of the sediment is a product of erosion of crystalline bedrock during the cataclysm, then this number also provides an estimate for that average rate of erosion.

With that quantitative estimate for the average deposition rate during the cataclysm, let us return to the challenge of generating uniform sediment layers on the order of 1,000 km in lateral extent. Sediment deposition implies sediment suspension and transport. As a thought experiment let us consider a layer that extends for 1,000 km, or 10^6 m, in the direction of water flow and everywhere along its length has a deposition rate of 12 m/day or 1.4×10^{-4} m/s. Let us assume that flow is from left to right, that sedimentation is from particles settling out of suspension from the moving water column, and that at the point 1,000 km from the left edge there is no sediment left in suspension.

For a strip 1 m in width, we find that the amount of sediment per second required to be entering the left boundary is (10^6 m) x (1 m) x (1.4×10^{-4} m/s) = 140 m^3/s. If this sediment is being transported by water moving to the right at a speed of 20 m/s, the water column on the left edge must be transporting a vertical equivalent of 7 m of suspended sediment. At a distance of 500 km from the left edge the water column must be transporting 3.5 m vertical equivalent of suspended sediment. The amount drops to zero at the right edge. The percentage of sediment that a moving water column can maintain in suspension is typically 5-10% or less (Pierson 2005). Let us choose a value of 7%. This implies that at the left edge in this thought experiment the water column must be on the order of 7 m/0.07 =100 m (330 ft) high.

Note that the deposition rate 1.4×10^{-4} m/s used above was the time average over the entire 150-day 'prevailing' stage of the cataclysm and spatially averaged over the entire continental portion of the earth's surface. When the likelihood of significant time variation is taken into account, the peak sediment and water column heights are substantially higher. When the mechanism involves episodic tsunamis, the water column heights of necessity become much larger. Approximating each tsunami as a step function pulse one-fourth the duration of the interval between tsunamis means that the height of the water column during the pulse is four times the average value.

Such estimates are difficult for the human mind even to conceive. It is not easy to imagine pulses of water 400 m (1300 ft) high, carrying some 28 m of sediment in suspension, moving at 20 m/s (45 mph) across the continental surface of the earth, depositing on average 12 m (39 feet) of new sediment each day for a time span of 150 days. Yet that is the sort of water process the fossil-bearing sedimentary record we observe on the continents today constrained by the time scale of the Genesis text seems to demand! This is the glaring challenge that this research effort is endeavoring to resolve.

This challenge prompted the first author about twelve years ago to pursue a numerical modeling strategy as a beginning attempt to address the issue. Two previous papers (Baumgardner 2013; Baumgardner 2018a) documented the mathematical underpinnings and numerical methods in moderate detail. In brief, the approach has been to solve for the water flow across the earth's surface utilizing what are known as the shallow water equations (Vreugdenhil 1994) that enforce conservation of mass and a balance of forces on each cell in the computational grid. The shallow water equations are a version of the standard Navier-Stokes equations for fluid flow under the simplifying assumption that fluid depth is small compared with the horizontal scales of interest. The shallow water equations allow one to treat the water as a single layer with laterally varying surface height above a laterally varying bottom topography. In addition, over continental regions, where the water depths are much smaller relative to the deep ocean and where turbulence can be expected to arise because of high water velocities, the equations of open channel flow are added to track the suspension, transport, and deposition of any sediment present. Erosion is treated assuming that cavitation was the dominant mechanism under the conditions that prevailed during the Flood.

B. A crucial question: What drove the water flow?

Among the important issues for understanding the Flood is that of the process responsible for producing and maintaining the required water flow. In the investigations leading to the Baumgardner (2013) paper, several possibilities were explored, including bolide impacts in the ocean, torque from a close approach of a planetary body, and the tidal effects of such a close encounter. Of these three possibilities, it was found that only the third could conceivably drive the water flow strongly enough and over a large enough fraction of the earth's surface to generate sufficient sediment and distribute it over the land surface in any sort of pattern that might bear some resemblance to the actual sediment record. Even in that case it was necessary to postulate multiple near approaches, presumably by the same extraterrestrial body, during the brief time span of the Flood. It was hence deemed a less than satisfying proposition, even though it did provide a means for testing and validating the other aspects of the numerical machinery.

Following the 2013 ICC presentation, a colleague inquired if tsunamis generated by catastrophic plate tectonics during the Flood had been seriously considered as a candidate mechanism. Although I (Baumgardner) had briefly considered this possibility, I had dismissed it because I had thought the tsunami amplitude would be too small. However, prompted by my colleague's inquiry, I reexamined the idea and realized that if the locking interval of the subducting plate with the overriding plate were on the order of merely an hour, then a tsunami of staggering amplitude would be unleashed when the plates unlocked and slipped. To illustrate, a subducting plate moving at 2 m/s at a steep angle into the mantle and dragging the overriding plate locked to it downward over an interval of an hour (3,600 s) creates a V-shaped trench exceeding 6 km in depth. When the fault between plates no longer can sustain the accumulated stress, the plates unlock and the overriding plate rebounds elastically to its undeformed shape. The seawater that had filled the V-shaped trench is quickly heaved upward, and a huge tsunami is launched, one capable of traversing a continent!

How many such giant tsunamis might have occurred during the Flood? In today's oceans active subduction zones total some 62,000 km in length (Bird 2003). If during the Flood the total length of active subduction zone were 50,000 km, the average subduction segment length were 1,000 km, and the average locking interval were one hour, this would imply (50,000 km/1,000 km) = 50 events per hour, or an event somewhere on earth every 72 seconds. This is equivalent to 1,200 mega-tsunamis per day or 180,000 in a span of 150 days. This is a direct logical implication of catastrophic plate tectonics. I realized that this process indeed represented a potent mechanism for driving high velocity water motion during the Flood. Implementing this new feature in the numerical model was not difficult.

Results from this tsunami forcing mechanism were reported in Baumgardner (2018a) for the case of two continental configurations that were fixed in time and in Baumgardner (2018b) which included the realism of a dynamic continent motion history. Both studies found that the erosion of bedrock by the cavitation mechanism on continent margins by repetitive large tsunamis arising from rapid plate tectonics was sufficient to supply most of the currently observed sediment inventory on the continents. These studies also showed that the tsunamis were effective in transporting this sediment into the continent interiors, depositing the sediment in laterally extensive layers on generally smooth intermediate surfaces. Both studies included initial continental topographies that were low along the continent margins and increased smoothly toward the continental centers. The tsunami-driven sedimentation preferentially filled the lowest regions to yield a flatter and flatter continental surface as time into the simulation progressed. Astonishingly, the Baumgardner (2018b) study yielded a global sediment distribution pattern at larger scales remarkably similar to what exists on the earth today.

Is there any clear objective physical evidence for such intense tsunami activity in the earth's past? The answer is yes! If one takes seriously the account provided in the biblical text for the Flood, including its short duration, then guyots, which are submerged oceanic volcanos whose tops have been beveled away by erosion, provide compelling physical evidence for the reality of intense global tsunami activity during the Flood. The larger of two examples shown in Fig. 2 has a surface area of 384 km^2 or 148 mi^2. To bevel away the top of a basaltic volcano during the short time span of the Flood requires extraordinary erosive intensity. These flat-topped seamounts occur in all the earth's ocean basins except for the Arctic. Out of a worldwide total of about 300, some 200 occur on the Pacific Ocean floor alone.

III. APPROACH

This present investigation also assumes that tsunamis, generated by the locking, and subsequent unlocking, and slip of the plate that overrides a rapidly subducting lithospheric slab in oceanic subduction zones, were the primary mechanism for driving water motion during

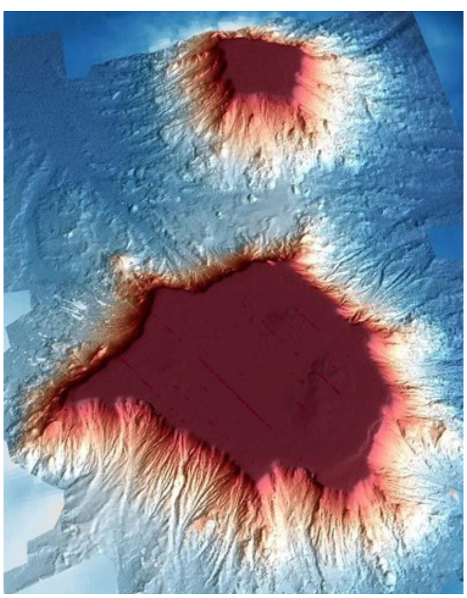

Figure 2. Examples of guyots, or tablemounts, which are submerged oceanic volcanos whose tops have been beveled away by erosion. The Gifford guyot and an unnamed one above it in this image are located in the southern Coral Sea, approximately 700 km east of Brisbane, Australia (Nanson et al., 2018). These seamounts have a depth range of approximately 3 km, rising from -3400 m on the abyssal plain to -250 to -350 m across their summits, and are dated to the Middle Miocene (Heap et al., 2009), that is, near the end of the Flood cataclysm. The plateau surface area of the Gifford guyot is 384 km^2.

the Flood. In today's subduction zones, the overriding plate is locked against the adjacent subducting oceanic plate except for extremely brief episodes of rapid unlocking and slip. As documented by GPS measurements (Prawirodirdjo and Bock 2004), this locking and episodic slip of the overriding plate takes place while the subducting plate is moving continuously downward into the mantle below. Relative motion between the subducting plate and overriding plate occurs only during those extremely brief intervals as the two plates suddenly unlock and slide rapidly past each other. In almost all cases today the episode of slip produces an earthquake and often also a tsunami.

In the context of the Flood, when the plates were moving approximately a billion times faster than they are at present, a crucial issue is the nature of the subduction zone mechanics. Until recently, no one had undertaken a careful numerical investigation of the dynamics in these zones under such conditions. During the past year preliminary numerical results indicate that lithospheric slabs do behave as assumed in previous modeling, even when the deformation rates are a billion times higher. It is expected that these results will be presented as a poster at this meeting.

Studies of plate motions during the Flood yield plate speeds on the order of 2 m/s (Baumgardner 1994; Baumgardner 2003). Using that surface speed for the subducting plate and assuming a subduction angle of 60° implies that the ocean bottom in the subduction zone is being pulled downward at a speed of $2 \text{ m/s} \sin(60°) = 1.73$ m/s. If the locking persists for 60 minutes (3,600 s), the sea bottom is depressed by some 6235 m. Sudden unlocking and slip between the overriding plate and the subducting plate will cause the sea bottom to rise by that height, unleashing a huge tsunami. Globally during the Flood, it is likely that subduction zones were comparable in linear extent as today, on the order of 60,000 km. If, as shall be assumed, there are 40 active subduction zone segments, each about 1,250 km in length, for a total active length of 50,000 km, and if each of these segments were locked and then slipped every 60 minutes, this would imply 40 mega-tsunamis unleashed each hour, 960 each day, and 144,000 over the course of five months in the world's ocean basins. These are the tsunami parameters assumed for the calculation reported in the Results section below.

The erosive power of these waves as they strike the continental margins and then race largely unhindered across the continental surface is difficult for the human mind to imagine. The turbulence where the water is relatively shallow over the continental surface is strong enough to maintain many tens of meters of sediment in suspension. Turbulence is the physical mechanism that enables the suspension and makes possible the long-distance transport of the sediment. Subsequent discussion of the numerical results reveals that these processes are readily adequate to account for major aspects of the Flood sediment record.

A. Mathematical framework

Prominent features of the sediment record suggest that sheets of turbulent water sweeping over the continent surface must have played a key role. Such water motion is in the general category of turbulent boundary layer flow, which is one of great practical interest and one that has been studied experimentally for many years. In the hydrologic engineering community, this type of water flow is referred to as open channel flow. Examples of open channel flows include rivers, tidal currents, irrigation canals, and sheets of water running across the ground surface after a rain. The equations commonly used to model such flows are anchored in experimental measurements and decades of validation in many diverse applications. It is the turbulence of the flowing water in such flows that keeps the sediment particles in suspension. The *Journal of Hydraulic Engineering* is but one of several journals that has published a wealth of papers on turbulent open channel flow and sediment transport over the past many decades.

Appendix A in Baumgardner (2018a) summarizes the observations, experiments, and efforts to formulate a mathematical description of fluid turbulence over the past two centuries. A description of turbulent fluid flow provided almost a century ago by the British scientist L. F. Richardson (1920) is still valid today. His description is a flow whose motions are characterized by a hierarchy of vortices, or eddies, from large to tiny. These eddies, including the large ones, are unstable. The shear that their rotation exerts on the surrounding fluid generates smaller new eddies. The kinetic energy of the large eddies is thereby passed to the smaller eddies that arise from them. These smaller eddies in turn undergo the same process, giving rise to even smaller eddies that inherit the energy of their predecessors, and so on. In this way, the energy is passed down from the large scales of motion to smaller and smaller scales until reaching a length scale sufficiently small that the molecular viscosity of the fluid transforms the kinetic energy of these tiniest eddies into heat.

When a fluid is moving relative to a fixed surface, the speed of the fluid, beginning from zero at the boundary, increases—first rapidly, and then less rapidly—as distance from the surface increases. The region adjacent to the surface in which the average speed of the flow parallel to the surface is still changing, at least modestly, as one moves away from the surface is known as the boundary layer. When the speed of the fluid over the surface is sufficiently high, the boundary layer becomes turbulent and becomes filled with eddies that can span a broad range of spatial scales. Appendix B in Baumgardner (2018a) summarizes some of the prominent features of turbulent boundary layers, including the discovery that the mean velocity profile within the turbulent boundary layer is very close to a logarithmic function of distance from the boundary. Remarkably, the parameters specifying the profile can be determined merely from the thickness of the layer and its mean flow speed.

The theory of open channel flow applies this mathematical representation of a turbulent boundary layer to describe sediment suspension, transport, and deposition by turbulent water flow for cases where the width of the flow is much greater than the water depth. Appendix C in Baumgardner (2018a) provides the derivation of a mathematical expression for the sediment carrying capacity of a layer of turbulent water as a function of sediment particle size. This expression is utilized in the numerical treatment to quantify the sediment suspension of the water flow. The expression requires the particle settling speed for each of the particle sizes that is assumed in the model. Appendix D in Baumgardner (2018a) describes how these settling speeds may be obtained via empirical fits to experimental data.

Obviously, a prominent issue in the formation of the earth's sediment record is the origin of the sediment. From the rock record it is clear that there were pre-Flood continental sediments. However, for sake of simplicity, these sediments are ignored in the current version of the model. Instead, it is assumed that all the sediment deposited is derived from erosion of continental bedrock. In terms of erosional processes, we restrict the scope to the mechanism of cavitation, again for simplicity. We suspect, however, that contributions from other processes by comparison were small. We further assume that the cavitation erosion of crystalline continental bedrock results in a distribution of particle sizes corresponding to 70% fine sand, 20% medium sand, and 10% coarse sand. Here the fine sand fraction also includes the clay and silt, which are assumed to flocculate to form particles that display settling behavior identical to that of fine sand. Mean particle diameters for these three size classes are 0.063 mm, 0.25 mm, and 1 mm, respectively. In this model we neglect carbonates which in the actual rock record represent on the order of 20-30% of the total sediment volume.

We recognize that it is difficult to imagine how feldspar in the continental crustal bedrock, even when reduced by cavitation to 0.063 mm particle sizes and smaller, might be transformed to clay minerals in the brief time span available during the Flood. We acknowledge that a significant portion of the clay in the shales and mudstones in the Phanerozoic sediment record may well have been derived from shales and mudstones of the pre-Flood earth. For example, the Precambrian tilted strata exposed in the inner gorge of the Grand Canyon, rocks that include the Unkar Group, the Nankoweap Formation, and the Chuar Group, display total thicknesses of about two miles, mostly of shale and limestone (Austin 1994). Even more impressive, the Mesoproterozoic (Precambrian) Belt Supergroup, exposed in western Montana, Idaho, Wyoming, Washington, and British Columbia, is mostly mudstone (shale, fine sand, and carbonate) and up to 8 miles in thickness (Winston and Link 1993). These examples hint that there may have been a vast quantity of mudrocks on the pre-Flood earth, possibly enough to account for most of the clay and carbonate rocks in the Flood sediment record. Exploring the consequences of initial conditions that include a substantial layer of pre-Flood mudstone sediments is an attractive task for future application of this model.

Appendix E of Baumgardner (2018a) provides a description of the cavitation submodel. It is implemented in the numerical code by means of a single equation involving three adjustable parameters. One of these parameters is the cavitation threshold velocity. For the calculation described in this paper, that threshold velocity is set to 15 m/s, below which no cavitation, and hence no erosion, occurs. Appendix E also describes the criteria for deposition and for erosion of already deposited sediment.

Given that the average thickness of Flood sediments on the continents today is about 2,000 m, it is not surprising that a numerical model capable of eroding, transporting, and depositing that much sediment will yield sediment thicknesses in some locations that significantly exceed that average value. In early tests it was found that the calculations become unstable unless some degree of isostatic compensation is allowed in locations where the sediment thicknesses become large. Appendix F in Baumgardner (2018a) describes how isostatic compensation is included in the two studies published in

2018. The scheme chosen here provides much more aggressive and realistic compensation. It applies 20% compensation for loads less than 200 m and increases to 50% compensation for the portion of the load between 200 m and 500 m. For the portion of load in excess of 500 m, 80% compensation is applied. Moreover, symmetrical compensation is implemented for the negative loads produced by material removed by bedrock erosion. Note that the compensation is instantaneous and that the fraction of compensation increases with increasing sediment load height. The assumption that the compensation is instantaneous would, at first, seem difficult to justify, even as an approximation. However, when one takes into account the extreme reduction in rock strength throughout the mantle caused by the stress weakening mechanism associated with runaway lithospheric slabs and mantle plumes, it becomes more plausible. Dynamical calculations show that the weakening, which starts in the vicinity of a slab or plume that is entering the runaway regime, quickly spreads to encompass the entire mantle. The reduction in rock strength throughout the mantle then approaches a factor of a billion. This reduction in rock strength also affects the lithosphere. It implies that a rapid response of the continental lithosphere to surface loading during the Flood while the mantle is in its weakened state is likely.

To describe the water flow over the earth in a quantitative way, the numerical model makes use of what is known as the shallow water approximation. This approximation requires that the water depth everywhere be small compared with the horizontal scales of interest. The depth of the ocean basins today—and presumably also during the Flood—is about four kilometers. By contrast, the horizontal grid point spacing of the computation grid for the case described in this paper is about 60 km, half that of the 2018 studies. The expected water depths over the continental regions, where our main interest lies, are yet much smaller than those of the ocean basins. Hence the shallow water approximation is entirely appropriate for this problem. That approximation allows the water flow over the surface of the globe to be described in terms of a single layer of water with laterally varying thickness. What otherwise would be an expensive three-dimensional problem now becomes a much more tractable two-dimensional one.

Appendix G in Baumgardner (2018a) outlines the mathematical approach for solving the shallow water equations for the water velocity and water height over the surface of the earth as a function of time. These equations express the conservation of mass and the conservation of linear momentum. They are solved in a discrete manner using what is known as a semi-Lagrangian approach on a mesh constructed from the regular icosahedron as shown in Fig. 1 of Baumgardner (2018a).

In this numerical treatment, a separate spherical coordinate system is defined at each grid point in the mesh such that the equator of the coordinate system passes through the grid point and the local longitude and latitude axes are aligned with the global east and north directions. The semi-Lagrangian approach, because of its low levels of numerical diffusion (Staniforth and Cote 1991), is also used for horizontal sediment transport. Over the continents seven layers of fixed thickness are used to resolve the sediment concentration in the vertical direction, with thinner layers at the bottom and thicker layers at the top of the column. This semi-Lagrangian method in the framework of the icosahedral mesh using local spherical coordinates has been applied and validated in one of the world's foremost numerical weather forecast models, a model known originally as GME and now ICON (for icosahedral non-hydrostatic), developed by the German Weather Service in the late 1990s (Majewski et al. 2002). The code that incorporates these many numerical features specifically for modeling the hydrological aspects of the Genesis Flood has been named 'MABBUL.' That word, of course, is the one used exclusively for the Flood in the Hebrew Old Testament.

B. Accounting for continent motion history

The original study (Baumgardner 2013) as well as a subsequent one (Baumgardner 2018a) utilized a single static continent. The study reported at the previous ICC (Baumgardner 2018b) added a displacement history for the various continental blocks spanning, in terms of geological nomenclature, the Paleozoic, Mesozoic, and Cenozoic eras, that is, the portion of the geological record formed during the Flood.

It is to be noted that, while the reconstruction of continent motions since the early Mesozoic has relatively small uncertainty because of the abundance of constraints from the present-day ocean floor, the motions during the Paleozoic typically have much more uncertainty because of the lack of surviving Paleozoic seafloor. The primary observational data for recovering the Paleozoic continent motions therefore are from paleomagnetism. Magnetic minerals in igneous rocks, provided that the rocks have not been significantly reheated since they crystalized, can record the orientation of the earth's magnetic field when the rocks crystallized. By measuring the magnetic declination and inclination in suitable igneous rocks from many points through the geological record for a given continent, one can construct a paleolatitude history for the continent. This procedure unfortunately provides no information on paleolongitude.

Paleomagnetic determinations were first undertaken in the late 1940s. By the early 1950s paleomagnetic 'polar wander paths' for Europe and North America were being published showing that both continents, relative to today's North Pole, had seemingly migrated northward dramatically since the mid-Paleozoic—by many tens of degrees. At the time this created quite a stir in the earth science community. In the decade of the 1960s, these paleomagnetic determinations helped convince many in the community that plates and plate mobility are indeed genuine realities. In subsequent decades more detailed and comprehensive paleomagnetic studies continued to reveal that same large amount of northward motion of Europe and North America relative to today's North Pole. The current estimated amount of northward motion is about 110°. From the vast number of paleomagnetic determinations now available from all the continents, secular geoscientists have been able to reconstruct the history of continental motion during the Paleozoic to what they believe to be a reasonable level of confidence despite the lack of strong longitude constraints in the paleomagnetic measurements.

Several secular authors (e.g., Scotese 2021; Blakey 2008) have now published continent motion histories that span the neo-Proterozoic to present. The work described in this present paper draws upon global paleogeography maps by both Scotese (2021) and Blakey (2008) as guides to that continent motion history. Fig. 3(a) is Blakey's map

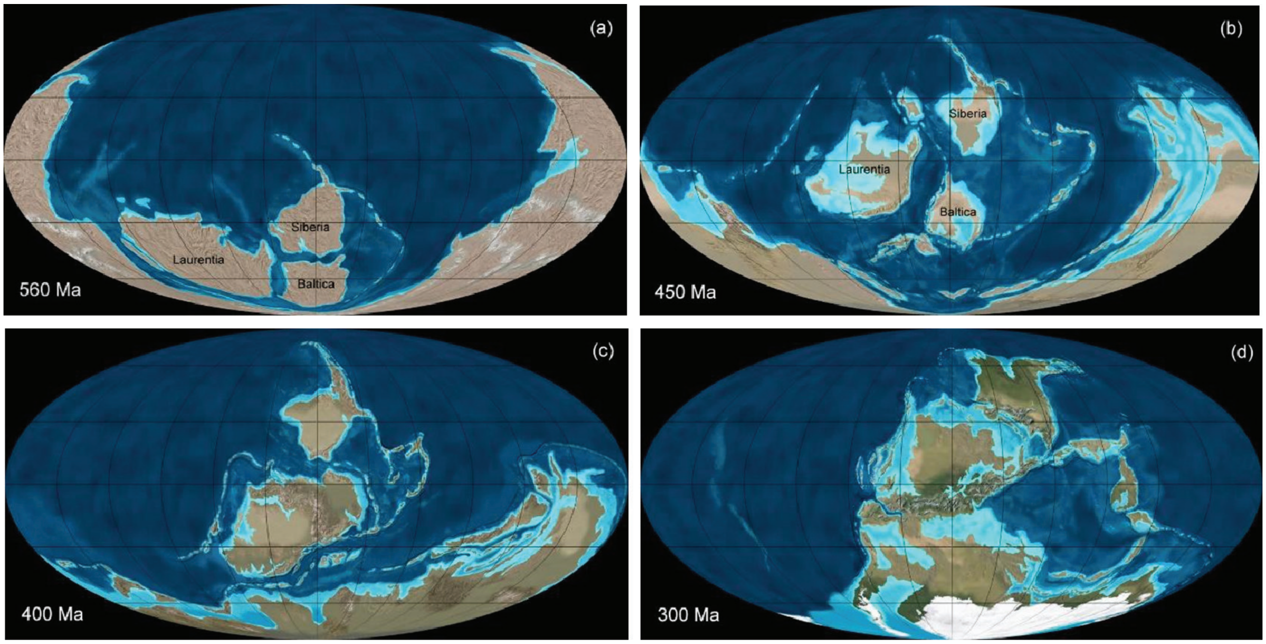

Figure 3. Selections from Ronald Blakey's (2008) set of global paleogeographic maps for times, in terms of the secular geological time scale, of 560 Ma (a), 450 Ma (b), 400 Ma (c), and 300 Ma (d). These snapshots show the breakaway of three continental block from the late Neoproterozoic supercontinent Pannotia and their subsequent re-amalgamation to form the early Mesozoic supercontinent Pangea.

for a time in the very latest neo-Proterozoic (560 Ma in terms of the secular time scale). In the time frame of the Flood this corresponds to very soon after the breakup of a pre-Flood supercontinent. Some, including the authors of this paper and Scotese, refer to the supercontinent as Pannotia. Others, including Blakey, refer to it as Rodinia. Note that the continental blocks Laurentia, corresponding to North America and Greenland, Baltica, corresponding to modern Western Europe, and Siberia, corresponding to Eastern Europe, have broken away from the rest of Pannotia, known as Gondwana, in a northerly direction. Although not shown explicitly in these maps, Gondwana consists of modern South America, Africa, Madagascar, India, Australia, and Antarctica as well as blocks that later become modern China and other portions of modern Asia. It is important to note that Gondwana, apart from the terranes that become modern China, persists intact throughout the Paleozoic to become part of Pangea.

Fig. 3 (b)-(d) are successive snapshots in time from Blakey's set of global paleogeography maps, snapshots that span most of the Paleozoic era. These show Laurentia, Baltica, and Siberia first moving away from the rest of Pannotia and from one another (b). They then show Laurentia and Baltica reversing directions relative to one another and colliding back together (c). Finally, they show the remainder of Pannotia moving northward in the eastern hemisphere, across the South Pole, and colliding with Laurentia/Baltica from the south and that assembly colliding with Siberia also from the south (d).

A major difference between the paleogeographical reconstruction of Scotese and that of Blakey involves a large displacement of Laurentia, Baltica, and Siberia relative to Gondwana during the early Paleozoic in Blakey's reconstruction as the three breakaway blocks come back together and rejoin Gondwana. That displacement is not that obvious in the plots of Fig. 3. The reconstruction by Scotese, however, eliminates this displacement entirely by having the initial locations of the three breakaway blocks in Pannotia relative to Gondwana the same as after they rejoin. Choosing these aspects of the Scotese reconstruction, as we choose to do, significantly reduces the required amount of Paleozoic subduction.

One can inquire as to the reliability of continent motion reconstructions such as those of Blakey and Scotese. My own assessment is that the basic features are robust. They are based on vast numbers of paleomagnetic determinations stretching back more than 60 years by many investigators for all the continents. They are also based on a vast amount of geological field observation, including indisputable evidence for continent-continent collisions during the Paleozoic and associated orogenies, for example, the Caledonian orogeny involving Europe and North America, the Variscan/Hercynian/Appalachian orogeny involving Europe, North America, and Africa, and the Uralian orogeny involving Europe and Asia/Siberia. While details remain uncertain, to us as authors there is little reason to question this overall displacement history.

C. The issue of polar wander

But what about the inferred 110° of motion relative to today's North Pole, not only for North America and Europe, but also for all of the other continental blocks since the beginning of the Paleozoic? In terms of the Biblical framework with its clear account of a global Flood cataclysm, it is nigh to impossible to conceive of all the continents migrating across the face of the earth, more or less in synchrony, for more than a quarter of the earth's circumference during the few months of the Flood. A much simpler explanation instead is that a change in the orientation of the earth's magnetic poles relative to the continents occurred during that interval, a phenomenon known in earth science circles as true polar wander. With this simpler explanation the 110° of actual continental motion disappears. This was the approach taken in the earlier Baumgardner (2018b) paper and the one we take in this paper as well.

Let us consider this topic in a bit more detail. Interpreting significant changes in paleomagnetic latitude as apparent polar wander implies that the magnetic poles remain largely fixed relative to the solid earth while the continents move significant distances across the earth's surface. By contrast, allowing for a significant amount of true polar wander, where the magnetic poles themselves migrate relative to the solid earth itself, requires dramatically less actual continental motion—over distances that can readily be understood in terms of normal plate tectonics processes. So the issue at hand, especially when one is dealing with measured changes in paleolatitude as large as 110°, is whether the magnetic poles have remained largely fixed relative to the earth's surface and the continents have actually migrated by vast distances, or whether the continents have moved relatively little and the magnetic poles themselves have moved by large distances. When one considers the brief time span of the Flood, this issue, of course, is accentuated. Indeed, it is difficult to conceive of a means by which the huge Gondwanan continent, which remained intact throughout the entire Paleozoic, might have plowed its way around the earth by more than a quarter of the earth's circumference in the time span of only a few months.

If one chooses the option of true polar wander, the question then arises as to what might have caused such rapid polar wander. The answer almost certainly involves the earth's rotational characteristics, namely, changes in the relative magnitudes in the earth's moments of inertia. Such changes could well have been produced by changes in the earth's internal density distribution, for example, by transit of a significant volume of cold lithosphere from the earth's surface into the deeper mantle and transit of a comparable volume of hot mantle rock from the core/mantle boundary into the mid and upper mantle. If sufficiently large, such changes indeed are able to alter temporarily the earth's rotational moments of inertia, leading briefly to a modest amount of rotation of the solid earth about one of its other principal axes. It is helpful here to emphasize that during an episode of true polar wander orientation of the earth's spin axis in space remains entirely fixed, and the earth's angular momentum remains perfectly conserved.

What happens when one assumes that the large changes in magnetic latitude are the consequence of true polar wander and not apparent polar wander? Investigating this question in his studies leading to his (2018b) paper, Baumgardner made an astonishing discovery. He found that rotating Pannotia 110° clockwise about an axis perpendicular to the plane, when viewed from the east, defined by today's zero degrees longitude meridian that runs through Greenwich, England, maps the Gondwanan continents in Pannotia, apart from the blocks that formed China, almost perfectly onto those same Gondwanan continents in Pangea! Baumgardner therefore made the bold assumption that, between the onset of the Flood and the point during the Flood when Pangea had assembled, this 110° of true polar wander indeed had occurred. This implied that during the first half of the Flood what today are the continents of Africa, South America, Antarctica, and Australia, plus India and Madagascar had remained stationary on the earth's surface. They experienced no displacement on the solid earth whatever during the entire Paleozoic part of the record. Moreover, the continents of North America and Europe plus the Siberian portion of Asia, apart from short Paleozoic excursions, also were at the same locations on earth in Pangea as they were in Pannotia at the onset of the Flood. Hence, the continental blocks forming Pangea, apart from the blocks that formed China, were essentially identical in their shapes and locations on the solid earth as they were in Pannotia at the onset of the Flood. We make this very same assumption in the current paper.

Pertaining to this issue, a reviewer who views Rodinia as possibly equivalent to Pannotia asked if we might comment on the following claim by Clarey (2020, pp. 159-160):

> A pre-Flood world that resembled Rodinia would require the consumption of nearly all the pre-Flood ocean crust twice. The first time would be while the continents from Rodinia moved into the configuration of Pangaea, and then a second time when Pangaea split into the present global configuration. Geophysically, the first break-up of Rodinia and reconfiguration into Pangaea would be possible, but it would also consume all of the dense pre-Flood ocean crust. A second move would then be rendered impossible since any significant amount of new ocean crust created while splitting up Rodinia would not have enough energy density contrast to fuel a second episode of subduction.

Our response is that assuming some 110° of true polar wander during the early portion of the Flood allows us to begin from a pre-Flood continent configuration that is essentially identical to Pangea in its location on the earth and its internal constitution (apart from the terranes that eventually form eastern Asia). This effectively eliminates the problem Clarey is describing! Moreover, it allows us to exploit the vast number of paleomagnetic determinations acquired over the past 70 years to obtain what we conclude is a reliable history of the continent motions for the Paleozoic portion of the Flood rock record.

We therefore utilize the paleogeographical reconstructions of Blakey and Scotese as our guide for obtaining the relative motions of the continental blocks as a function of time during the earlier portion of the Flood. Since true polar wander affects all these blocks identically, it is legitimate to use reconstructions such as these as a guide for the relative motions.

Introduction of true polar wander into the model means that points on the earth's surface change with time relative to the orientation of the earth's spin axis in space. To account properly for the Coriolis effect in the numerical formulation that utilizes a computational grid fixed with respect to the solid earth, we need merely to alter the orientation of the spin axis appropriately with respect to the computational grid in the numerics. This requires only a trivial change in the coding to allow the orientation of the spin axis to change with time in a prescribed way.

D. Including continent motion history in the numerical model

How does one actually incorporate a specific continent motion history into a numerical model? The approach we have taken utilizes an explicit description of the motion of each continent block as a function of time. As described in Baumgardner (2018b) this is accomplished by specifying rotation poles for each of 11 different continental blocks for each of 10 separate time intervals. Each rotation pole is a vector in space with three components (x, y, z) that specifies the rate of displacement of the rigid block over the surface of the sphere during the time interval. As might be surmised, obtaining those rotation poles guided by the paleogeographic maps is a moderately tedious process. Fig. 4 provides snapshots from the resulting time history. Green regions denote continent, while blue regions correspond to deep ocean. The continental configuration for the time of 0 days corresponds to Pannotia at the onset of the Flood, while the continent configuration at a time of 90 days corresponds to Pangea. The primary difference between Pannotia and Pangea in this model is the location of the land area that today corresponds to eastern Asia. In Pannotia this land area adjoins Gondwana along its northeastern boundary. In secular continent motion histories this land area is also similarly adjoined to Gondwana, but splits away in multiple, successive slices that migrate northward and coalesce to become eastern Asia. In our treatment we omit the complexity of the multiple slices, and instead combine those slices into a single block. Again, by assuming the latitude difference between Pangea and Pannotia is the result of true polar wander, Pannotia and Pangea, apart from eastern Asia, are essentially identical in their locations on the earth. This simple assumption eliminates the vast amount of plate motion and ocean floor subduction required by the secular models for Pannotia to be transformed into Pangea.

E. Generation of the tsunamis

As discussed earlier, we conclude that large tsunamis were the means by which the high water speeds for sustaining the high rates of erosion and sediment transport and deposition during the Flood were generated. For the example case to be shown later in this paper, zones of subduction are chosen to lie along three great circle arcs. These zones are divided into 40 distinct segments, averaging about 1,250 km in length. Subduction is assumed to be occurring at an angle of 60° into the mantle along each of these segments with the surface speed of the subducting plate assumed to be 2 m/s for the initial 150 days, after which it drops to 1 m/s until 180 days, and then to 0.5 m/s.

While the subducting and overriding plates are locked, the seafloor in the subduction zone is assumed to be moving vertically downward at a rate of 0.866 times the assumed surface plate speed because of the steady sinking motion of the subducting lithospheric slab. Each computational time step, corresponding to an interval 90 s or 1.5 minutes, one of the 40 segments is allowed to unlock and slip, allowing the bottom of the subduction zone trench to rebound to its nominal, undepressed height. Each individual segment therefore slips every 40 x 1.5 = 60 minutes. The amplitude of the rebound of the trench bottom is 6,235 m (2.0 m/s x 0.866 x 3,600 s). This impulsive uplift of the segment of trench bottom initiates a tsunami that travels across the 4,000-m deep ocean at a speed of about 200 m/s. Note that tsunami wave speed is given by $(gh)^{1/2}$, where g = 9.8 m/s^2 is the gravitational acceleration and h is water depth. The generation rate of one tsunami every 1.5 minutes is equivalent to 960 per day and 144,000 over a time span of 150 days. Initially the water is assumed to be at rest with its surface at sea level.

F. The imperative of supernatural cooling of the ocean lithosphere during the Flood

In his very first paper on catastrophic plate tectonics Baumgardner (1986) stressed that conductive cooling of the entirety of today's ocean lithosphere within the Biblical time frame lies outside the known physical laws and therefore almost certainly points to God's intervention in the laws of nature during the Flood cataclysm, as implied in 2 Peter 3:5-6. Subsequent 3D numerical modeling of the rapid plate tectonics of the Flood dealt with this issue simply by assuming a large value for rock thermal conductivity that allowed the earth's surface layer of rock to conduct heat at a suitable high (but physically implausible) rate (Baumgardner 1990; Baumgardner 1994). That approach in effect inserted God's intervention for cooling the newly forming ocean lithosphere, at the rate required by the Genesis text, into the numerical calculations.

For this present study it is helpful to address the requirement for enhanced cooling of the ocean lithosphere in a more explicit and quantitative manner. Assuming the rate of creation of new ocean lithosphere at spreading ridges matches the rate of subduction of ocean lithosphere, the rate of creation of new ocean floor is the product of the total length of active subduction zones and the average plate speed. Estimating the total length of active subduction zones during the Flood to be 50,000 km and the average plate speed to be 2 m/s, we obtain an estimate for the rate of creation of new ocean floor to be (50,000 km) x (0.002 km/s) = 100 km^2/s or $8.64x10^6$ km^2/day. This yields an estimate for the total amount of new ocean lithosphere formed during the 150 days of the 'prevailing' stage of the Flood (Genesis 7:24) of (150 days) x ($8.64x10^6$ km^2/day) = $1.3x10^9$ km^2.

Note that this total far exceeds the total surface area of the ocean basins, which is about 70% of the earth's surface area. The latter number, given by $4\pi r_e^2$, where r_e is the earth's radius, is (4 x 3.14) x $(6{,}370\ km)^2$ = $5.1x10^8$ km^2. The area of the ocean basins then is 70% of that number, or $3.57x10^8$ km^2. Note that at a rate of $8.64x10^6$ km^2/day, the entire ocean bottom is subducted and replaced with new hot ocean floor after only ($3.57x10^8$ km^2) / ($8.64x10^6$ km^2/day) = 41.3 days into the Flood. The elevated temperature profile of thin, newly formed ocean lithosphere makes it effectively unsubductable. Were hot lithosphere to cover the entire ocean bottom, subduction would cease and the CPT process would come to an abrupt halt. This illustrates the imperative of a vast amount of active supernatural cooling of the ocean lithosphere during the Flood. The question then arises, was this lithospheric cooling uniform in time as has been assumed in previous numerical simulations, or was it possibly pulsed in time? We shall observe shortly that there is evidence to infer that it was the latter.

G. Accounting for erosional discontinuities between stratigraphic megasequences

A landmark paper by L. L. Sloss in 1963 documented the reality of six large packages of fossil-bearing, sedimentary rock layers draped across North America, separated from one another by erosional unconformities spanning the continent (Sloss 1963). These packages are now referred to as megasequences. During the early 1980s the American Association of Petroleum Geologists undertook a massive project known as COSUNA (for Correlation of Stratigraphic Units

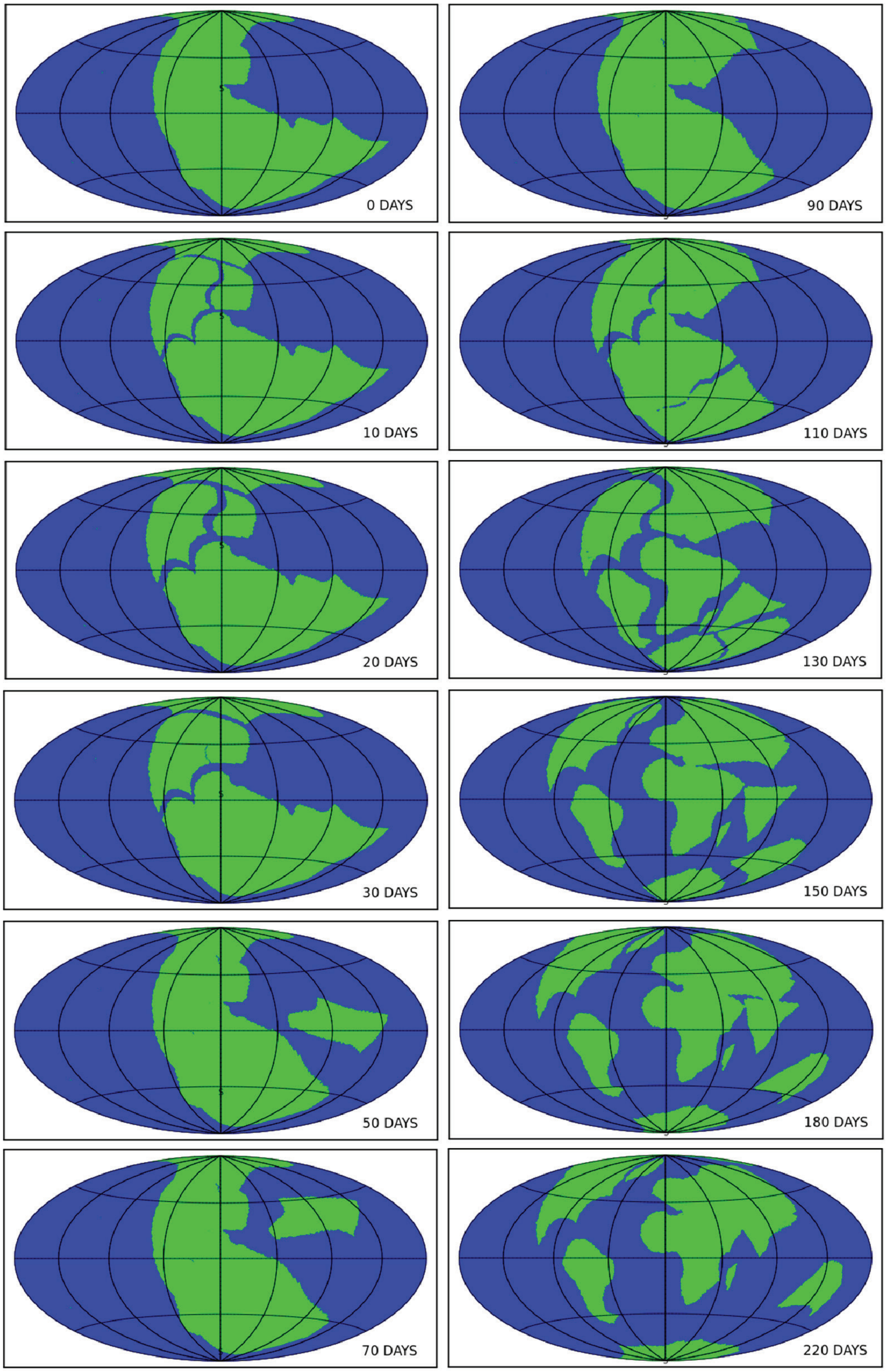

Figure 4. Snapshots in equal-area projection of the continent motion history assumed in this model at times of 0 days, 10 days, 20 days, 30 days, 50 days, 70 days, 90 days, 110 days, 130 days, 150 days, 180 days, and 220 days. True polar motion along the prime meridian is assumed to occur between the beginning of the simulated history until a time of 90 days. The North and South poles migrate in the plane defined by the prime meridian by 110° during this interval. The location of the South Pole is marked by the letter 'S.' The map projection is chosen such that Gondwana, which remains intact during that interval, is stationary. This means that in this projection the Africa block undergoes no motion from its original Pannotia location and its location as part of Pangea.

of North America) using data from drill-holes and from rock surface exposures to correlate and align rock layers in all the local sequences across North America (Lindberg 1986). The outcome was an overwhelming confirmation that the megasequences, as well as the erosional discontinuities between them, as described by Sloss two decades earlier, indeed were real. Subsequent investigations show that these megasequences are global in extent (Clarey and Werner 2017; Clarey 2020).

A major question associated with the discovery of this large-scale structure in the fossil-bearing stratigraphic record pertains to the mechanism responsible for generating the erosional unconformities separating the megasequences. The secular community's answer partly involves alternating periods of falling and rising sea level driven by fluctuations in the rate of seafloor spreading and consequent changes in the amount of warm, buoyant lithosphere adjacent to the mid-ocean ridges. During periods of more rapid seafloor spreading, the ocean bottom near the ridges is relatively higher due to the warmer rock beneath, the ocean basin volume is thereby reduced, and the global sea level is higher. During periods of relatively slower seafloor spreading the opposite prevails. The other part of the answer involves changes in what is known as dynamic topography that is driven by flow of rock within the mantle.

In the framework of the Genesis Flood and the rapid plate tectonics which it implies, fluctuations in the cooling rate of the new ocean lithosphere being generated by rapid seafloor spreading becomes a serious candidate explanation. As emphasized in the preceding section, a mechanism of enhanced cooling beyond that of thermal conduction seems to be a logical necessity. Allowing this mechanism to occur in pulses instead of in a uniform manner would plausibly account for sudden drops in sea level and global episodes of erosion of the continental sediments. Let us now explore that possibility in a quantitative manner to address the questions of how much sea level rise is implied by CPT and how large must the sea level drops be?

As mentioned above, 50,000 km of active subduction zones and an average plate speed of 2 m/s, implies a rate of creation of new ocean floor of (50,000 km) x (0.002 km/s) = 100 km^2/s or 8.64x10^6 km^2/day. If we assume that the thermal structure of subducting ocean lithosphere and also for newly forming lithosphere at a mid-ocean ridge to be similar to that of today, we infer a difference in sea bottom height from near a mid-ocean ridge and near a subduction zone of about 1,500 m (Solomon and Toomey 1992). From these numbers we can compute an estimate for the rate of ocean volume change arising from the CPT creation and subduction of ocean lithosphere. That rate is (8.64x10^6 km^2/day) x (1,500 m x 1 km/1,000 m) = 1.3x10^7 km^3/day.

One can express this rate of ocean volume change in terms of a rate of change in average sea bottom height. Since the deep ocean basins cover some 70% of earth's total surface area of 5.1x10^8 km^2, the rate of average sea bottom uplift corresponding to a global rate of ocean volume change of (1.3x10^7 km^3/day) is given by (1.3x10^7 km^3/day) / (0.7 x 5.1x10^8 km^2) = 0.036 km/day = 36 m/day.

Now let us consider the sort of sea bottom drops from episodes of lithospheric cooling that might be appropriate. Over a time span of 150 days, the total cumulative amount of sea bottom rise without cooling is (36 m/day) x (150 days) = 5,400 m. To account for all the erosional unconformities, we require seven episodes of sea level drop, one at the beginning, five separating the six megasequences, and one at the end. If for simplicity we make all the episodes of equal size, we find that by choosing each to result in a 700 m drop in the average sea bottom height, we account for 7 x 700 = 4,900 m, or most of the total sea bottom drop needed to match the total sea bottom uplift. To make these totals match, we include an additional 500 m to the final drop to make that drop, the one responsible for the Flood runoff, equal to a total of 1,200 m. Just prior to that final cooling episode beginning at day 150, the mean global sea level reaches its maximum value of 995 m. This is very close to the maximum height assumed in the initial topography as displayed in Fig. 5. We have incorporated these features into the MABBUL software. We model the first six of these sea level drops to occur at 25-day intervals beginning at time zero, with each unfolding during a 24-hour period. The final drop begins at a time of 150 days at a rate of 48 m/day and extends over 25 days, corresponding to the runoff stage of the Flood. Motivated by the large amount of seafloor with later Cenozoic age as well as flat-topped guyots also of later Cenozoic age, we include in the model ongoing seafloor spreading and tsunami generation between days 175 and 220, during which the resulting sea bottom rise is exactly compensated by sea bottom drop from cooling of the oceanic lithosphere. This results in a sea level at the end of 220 days that matches the modern one.

H. Candidate mechanism for the Great Unconformity

The case just presented for large pulses of cooling of the ocean lithosphere during the Flood brings with it a compelling candidate mechanism for the Great Unconformity. The Great Unconformity is the erosional discontinuity that marks the base of the Sauk Megasequence. This boundary is noteworthy in that it coincides with the abrupt appearance of fossils of multicellular organisms in the earth's rock record. As such it logically represents the onset of the Genesis Flood. In many places this erosional boundary displays evidence of extremely high-energy water flow. One example is in Devil's Lake State Park in south central Wisconsin as displayed in Fig. 6.

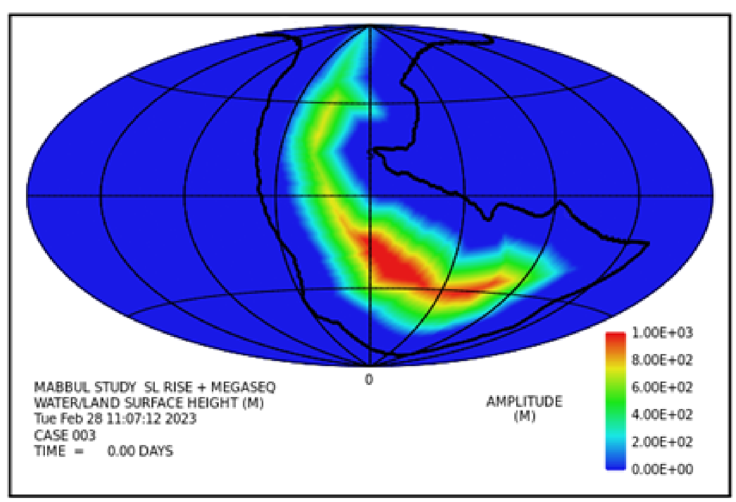

Figure 5. Initial topography assumed for the supercontinent Pannotia.

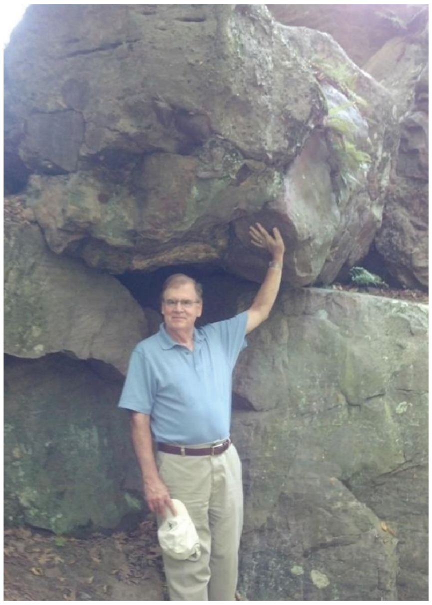

Figure 6. (Left) Large boulder of Baraboo Quartzite lying atop the massive Precambrian Baraboo Quartzite formation in Devil's Lake State Park in central Wisconsin. (Right) Additional Baraboo boulders at the same site. The boundary just beneath the boulder layer is the local expression of the Great Unconformity, the erosional discontinuity that marks the abrupt appearance of multicellular organisms in the earth's rock record. The intensity of the water process responsible for ripping up and transporting boulders of this size is almost beyond human comprehension.

Two ICC technical papers (Sigler and Van Wingerden 1998; Van Wingerden 2003) document the catastrophism associated with this boundary in an even more dramatic way. These papers summarize two masters theses on the pre-Flood/Flood boundary completed at Institute for Creation Research by Sigler in 1998 and Van Wingerden in 2000. These two authors document some 12,000 feet of catastrophic deposits thinning eastward just beneath the Sauk megasequence along the western edge of North America extending from Sonora, Mexico to the North Slope of Alaska. It includes spectacular detachment fault blocks, diamictite, tholeiitic volcanics, Ediacaran multicellular fossils, and salt strata.

Although most creationists are keenly aware of the reality and significance of the Great Unconformity, there seems to be no clear consensus on the actual mechanism by which it was formed. However, in the context of the discussion in the preceding section on the cause for the erosional unconformities that separate the megasequences, a reasonable inference emerges. It is that the same mechanism responsible for the erosional discontinuities between the megasequences also accounts for the Great Unconformity at the base of the first megasquence, namely, an episode of cooling of oceanic lithosphere by many hundreds of degrees Celsius and a consequent rapid drop in the global sea level by many hundreds of meters. Such an abrupt drop in sea level would have resulted in catastrophic runoff of water that covered the margins of Pannotia, producing the spectacular deposits we observe today, for example, along the western margin of North America. We therefore meekly offer this as the causal mechanism for the Great unconformity. With this possibility in view, we have included it in the illustrative simulation described below.

As emphasized above, God's cooling of the oceanic lithosphere has been an inherent component of the catastrophic plate tectonics framework since the first paper in 1986. Not until this paper have we suggested that this cooling occurred in distinct pulses. Because abrupt cooling of the ocean lithosphere increases its negative buoyancy and enhances its potential for runaway, a further consequence of the first pulse at the base of the Sauk megasequenceis that it might well have been the trigger that initiated the Flood tectonic cataclysm itself.

IV. RESULTS

We shall now present results from a case with the water motion driven by large-amplitude tsunamis that includes the continent motion history described earlier. The continent surface is assumed everywhere to consist of crystalline bedrock. The earth is assumed to be spinning at its current rate of rotation.

Understanding the results from the model is a challenge because of the model's many variable quantities such as water velocity, water depth, erosion rate, cumulative erosion depth, suspended sediment according to particle size for multiple particle size classes, deposited sediment according to particle size, and topographic height accounting for erosion, sedimentation, and isostatic adjustment, just to name a few. Each of these quantities varies both in time and potentially with respect to location across some 164,000 individual grid points that span the earth's surface. The only way a human being can possibly interact with such vast amounts of numerical information is for the information to be represented in a visual manner and then sampled only sparsely in time. Space restrictions in a written paper impose additional constraints.

With these considerations in view, we have chosen to include a relatively small set of color plots at a few points in time from the calculation to attempt to afford the reader the opportunity for at least a qualitative grasp of the model results. The times we have selected are at 20, 50, 80, 110, 150, and 200 days from the start of the simulation. Because the continent motion history in this model is similar to that derived by the secular geology and geophysics communities, it is possible to connect times in this model with corresponding points in the secular geological time scale. The continent configuration at 20 days corresponds to 470 million years ago in the secular geological time scale (early Ordovician), 50 days to 320 million years ago (early Pennsylvanian/mid-Carboniferous), 80 days 220 million years ago (late Triassic), 120 days to 150 million years ago (late Jurassic), 160 days to 60 million years ago (Paleocene), and 200 days to 10 million years ago (late Miocene).

Fig. 7 provides plots at 20 days for the surface height of either the water or land, whichever is greater, the cumulative depth of bedrock erosion, and the net cumulative depth of deposited sediment. Plots (a) and (b) clearly show water waves in the deep ocean with trough to crest amplitudes of well over 1,000 m! These waves correspond to

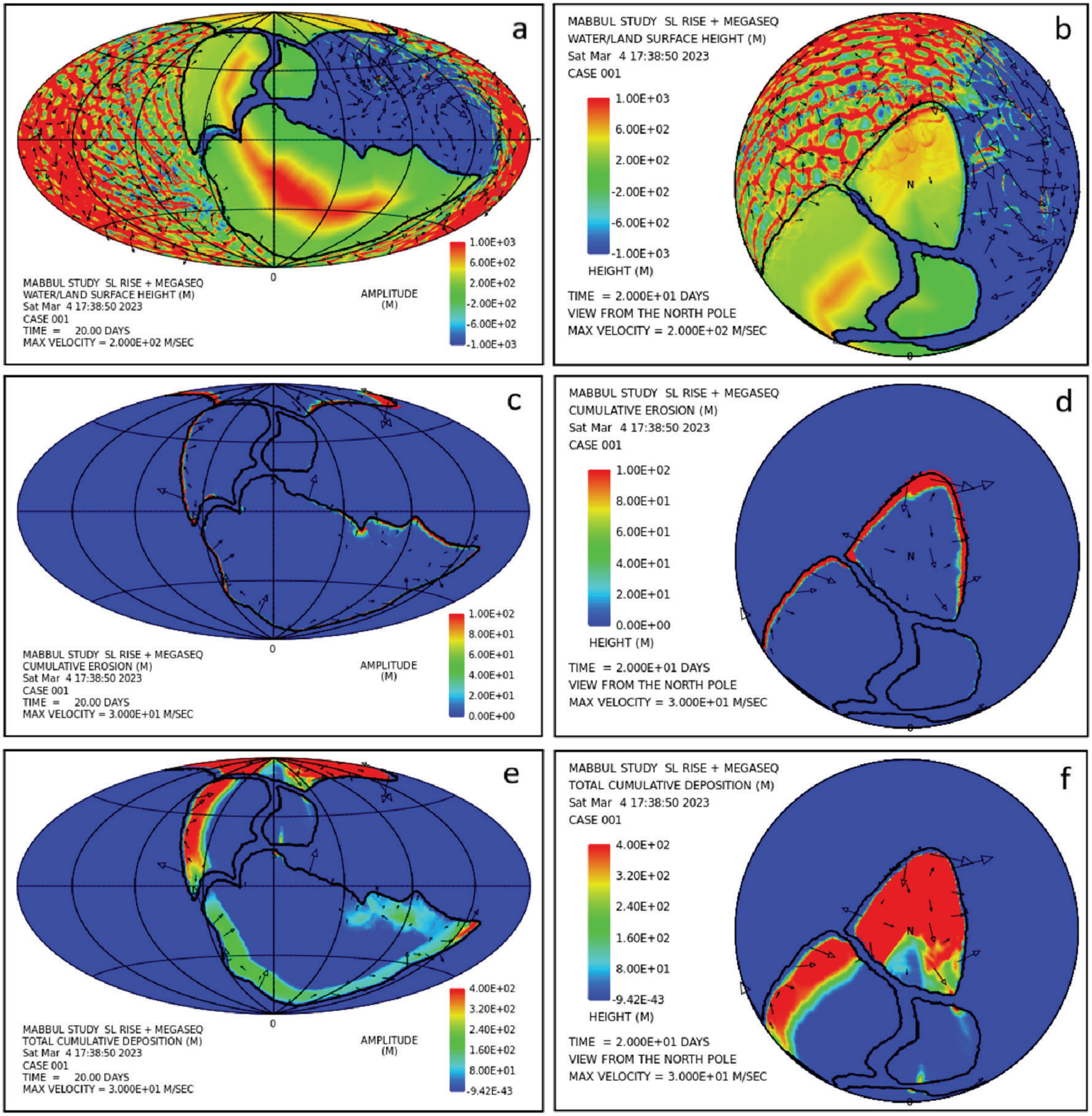

Figure 7. Plots in equal-area projection and geographic North Pole orthographic projection at 20 days of ocean or land surface height, whichever is greater, (a), (b); cumulative depth of bedrock erosion, (c), (d); and cumulative depth of deposited sediment, (e), (f). In (a) and (b) arrows denote water column velocities, clipped at 200 m/s. In (c)-(f) arrows denote water velocities just above the land surface, clipped at 30 m/s.

the tsunamis generated in a repetitive manner, every 60 minutes at a given location along active subduction zones. Such waves propagate at a speed of 200 m/s in the deep ocean. Plots (c) and (d) display the cumulative depth of crystalline bedrock erosion. As might be expected, the most intense erosion is occurring along the continent margins where the tsunami waves encounter the abrupt topographic change from deep ocean to continent. Plots (e) and (f) show the cumulative amount of sediment deposition of all sediment sizes. Regions of thick deposition generally occur in a band just inland from the coast. It is noteworthy that already at this stage in the simulation these zones in the coastal lowlands display sediment thicknesses of more than 300 m. At 20 days the average depth of bedrock erosion over the entire continent surface is 125 m. The average depth of sediment accumulation is 123 m, and the average amount of sediment in suspension is 2.2 m, where the averages are over the entire continental surface area. In all these plots the displacements of Laurentia, Baltica, and Siberia away from the remainder of Pannotia are evident.

Fig. 8 provides plots at 50 days of water/land surface height, cumulative depth of bedrock erosion, net cumulative depth of deposited sediment. By this stage in the calculation, Baltica and Laurentia have reversed direction and collided with each other, resulting in the Caledonian orogeny. That block has in turn collided with Gondwana, producing the Variscan/Hercynian/ Appalachian orogeny. Those prominent mountain belts are expressed in the model as enhanced topography in those continent collision zones. Siberia has also collided with Baltica and Laurentia such that Siberia, Baltica, Laurentia, and Gondwana are now all joined together in a manner very similar to their earlier locations in Pannotia. Notably, the portion of continent that is to become eastern Asia has broken away from what earlier had been northeastern Pannotia and is now moving northward. At this point in the calculation the south rotational pole has moved to approximately 50° south latitude (marked by S on the equal area plots) along the zero-longitude meridian. Plots (e) and (f) show that sediment continues to accumulate in the zones adjacent to the coasts and that the zones are tending to expand inland. At 50 days the average depth of bedrock erosion over the entire continent surface is 343 m. The average depth of sediment accumulation is 340 m, and the average amount of sediment in suspension is 3.4 m.

Fig. 9 displays the water/land surface height, the cumulative depth of bedrock erosion, and the net cumulative depth of deposited sediment at a time of 80 days. At this stage in the calculation, the east Asia block is near to docking with the Siberian block. That docking, which occurs at 90 days, will complete the assembly of Pangea. At 80 days there are regions where sediment thickness has reached well over 1,500 m. On average there is 581 m of erosion, 573 m of sediment over the land surface and 7.9 m of sediment in suspension.

Fig. 10 displays, at a time of 120 days, water/land surface height, cumulative depth of bedrock erosion, and net cumulative depth of deposited sediment. At this point in the calculation, the Pangean supercontinent is beginning to break apart. The present North Atlantic Ocean is opening as the northern portion of Pangea consisting of Laurentia and Eurasia rotates clockwise relative to Gondwana. The Gondwana block itself is beginning to rift apart along the eastern margin of what today is Africa. At this stage in the calculation the rotation axis matches today's orientation. The total volume of eroded sediment at this point is equal to an average of 825 m over the entirety of the continental surface.

Fig. 11 displays the same fields at a time of 160 days. At this point Gondwana has disassembled fully into blocks corresponding to South America, Africa, Madagascar, India, Antarctica, and Australia, and Laurentia has split away from Eurasia in the north. The average amount of sediment deposited on the continent surface is now 1225 m.

Fig. 12 displays the same fields at a time of 200 days. The continents are close to their current locations Water speeds are now small. The average amount of sediment deposited on the continent surface is 1486 m.

From these plots the vast amount of sediment being eroded from the continent margins and being suspended and transported into the continent interiors by the highly turbulent water is readily evident. Fig. 13 provides a more rapid sequence of snapshots to illustrate how a large pulse of water invades the continent up its sloping topography and then drains away leaving its sediment load behind.

Fig. 14 provides a comparison between the sediment distribution produced by this numerical model and the sediment distribution across the earth's surface today. To the authors, the overall agreement is astonishing. For example, apart from a zone across its north, Africa is largely barren of sediment. Similarly, India, northeastern Antarctica, western Australia, eastern South America, and northeastern Europe also display a paucity of sediment.

V. DISCUSSION

A. A big picture approach

Of necessity almost any attempt, and certainly this one, to model and understand how the Flood sediment record was generated during the global Genesis Flood must be a 'big picture' approach. As mentioned in the background section, one of the most acute challenges in this enterprise is accounting for the extreme rate of sediment erosion, transport, and deposition required, which is 12 m, or 40 feet, per day on average of the entire continental surface of the earth. The authors conclude that this numerical model demonstrates to a reasonable degree of confidence that the mechanism of tsunami-driven water flow as a consequence of catastrophic plate tectonics is able to account for such a high rate of sediment creation, transport, and deposition. The authors view this as the paramount 'big picture' result that we desire to communicate in this paper.

Another result we deem as significant is the sediment distribution pattern that the model produces. As summarized in Fig. 14, there is a notable similarity between the pattern of sediment distribution generated by the numerical model and the observed pattern of sediment distribution on the continents today. As to an explanation, it appears that this agreement in some measure reflects proximity to a coastline and hence to exposure to intense tsunami activity and the duration of that proximity. As such, this explanation relies to a significant degree on the validity of the motion history assumed for the continents.

A further result that bears emphasizing is that the sediment is on top of the continents, which themselves stand some 4,000 m above the

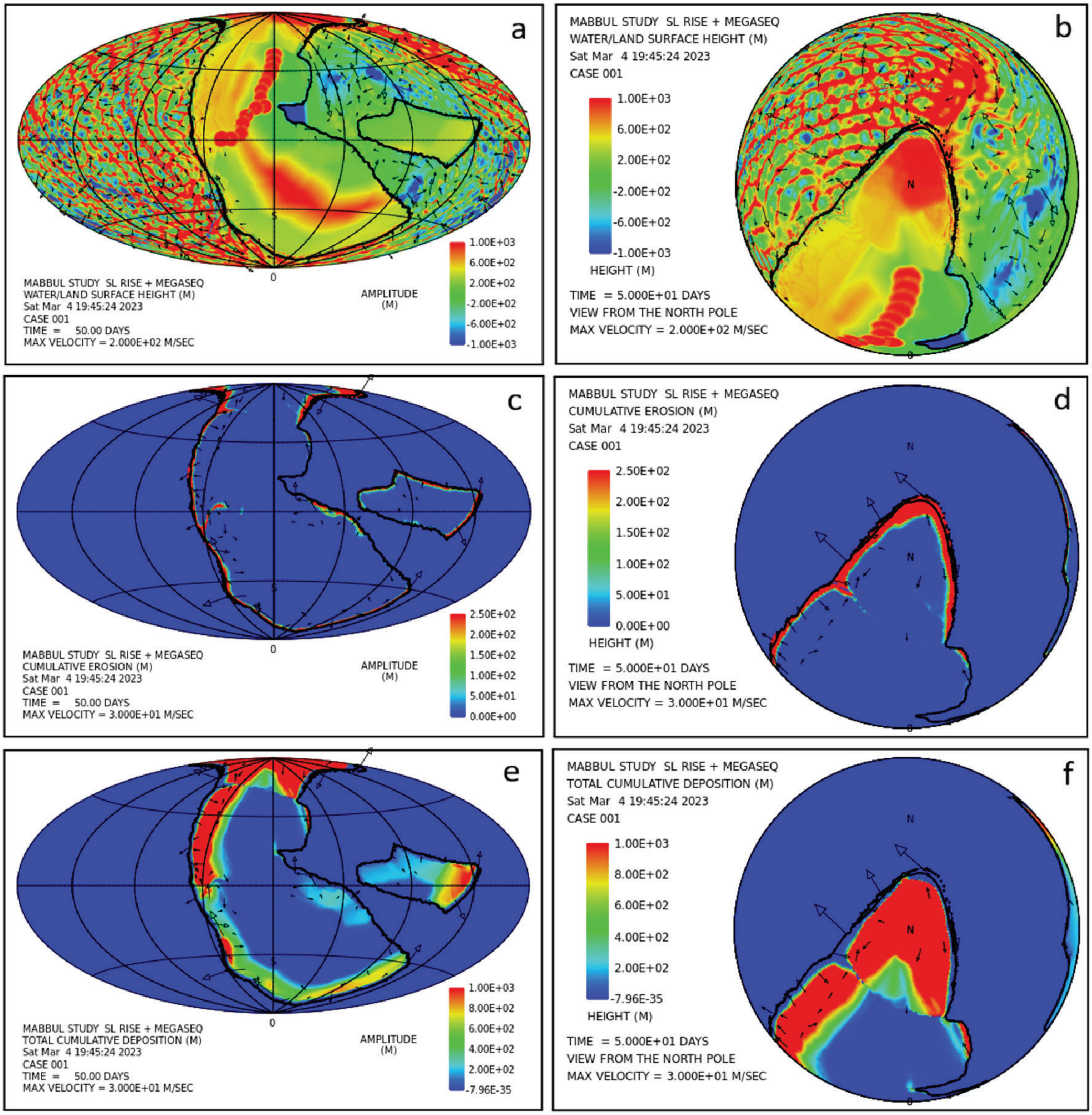

Figure 8. Plots at 50 days of ocean/land surface height (a), (b); cumulative depth of bedrock erosion, (c), (d); and cumulative depth of deposited sediment, (e), (f). Arrows denote water velocities as in Fig. 7. Mean sediment depth on the continental surface is 343 m.

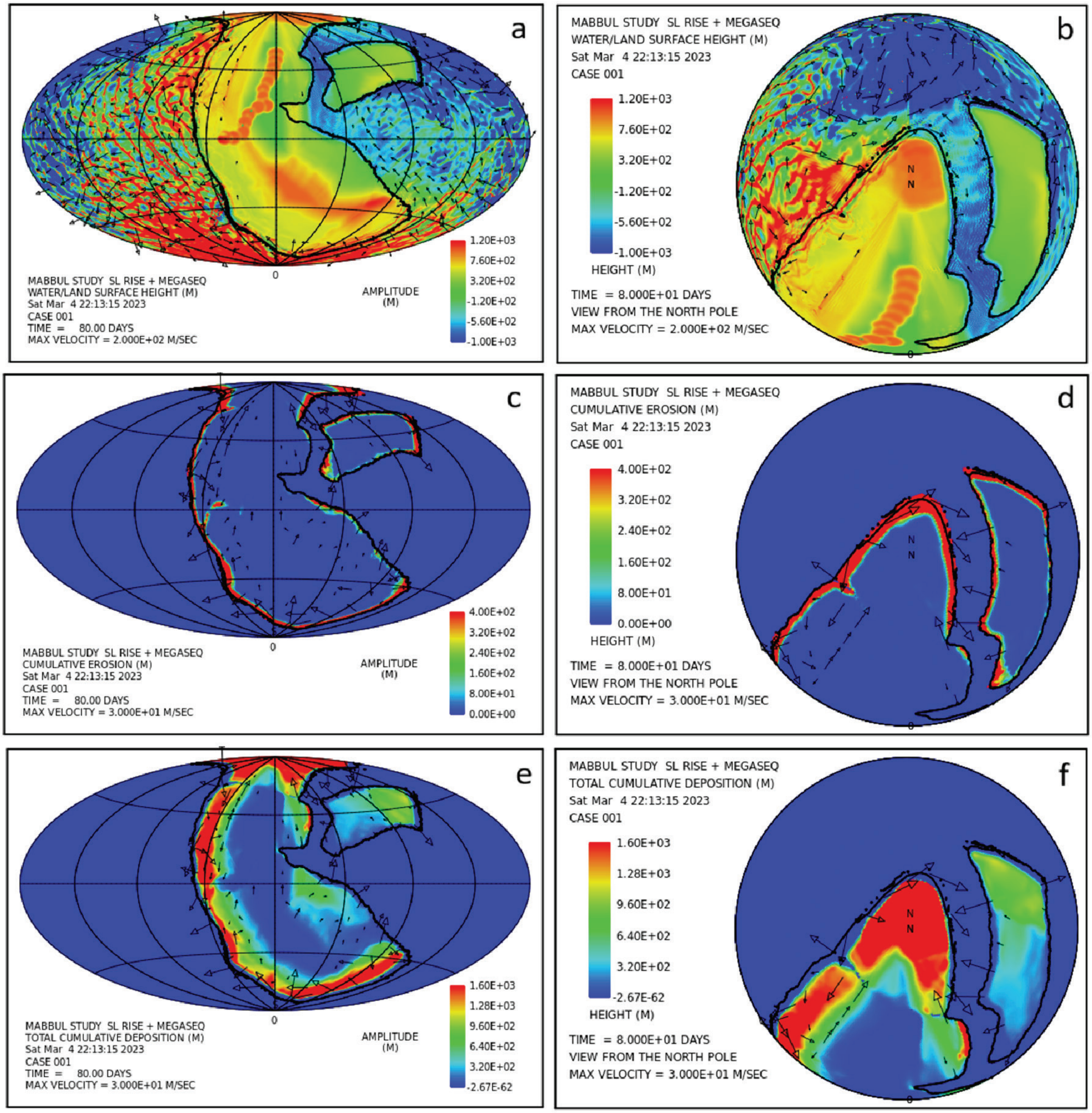

Figure 9. Plots at 80 days of water/land surface height (a), (b); cumulative depth of bedrock erosion, (c), (d); and cumulative depth of deposited sediment, (e), (f). Mean sediment depth is 581 m.

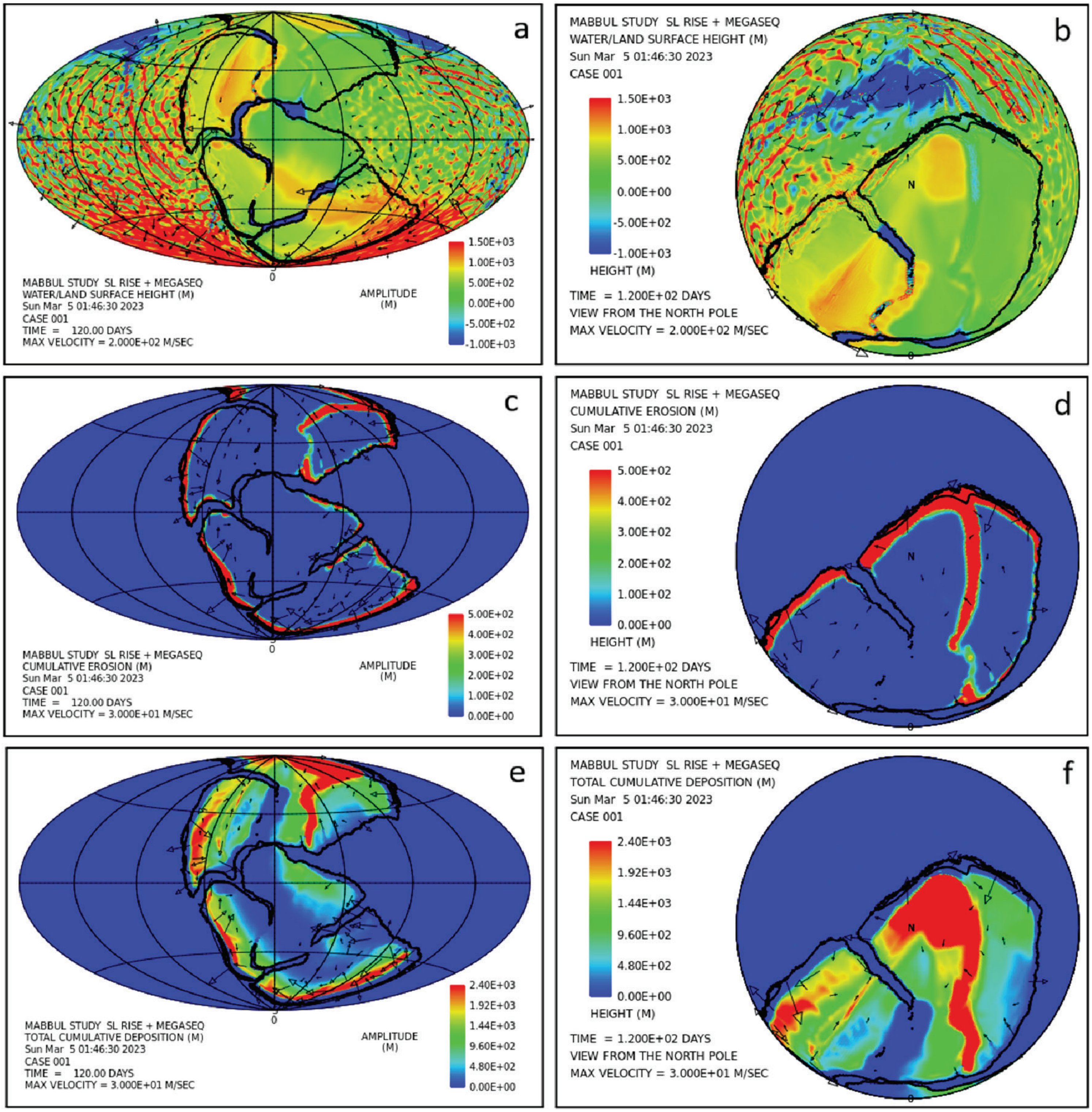

Figure 10. Plots at 120 days of water/land surface height (a), (b); cumulative depth of bedrock erosion, (c), (d); and cumulative depth of deposited sediment, (e), (f). Mean sediment depth is 825 m.

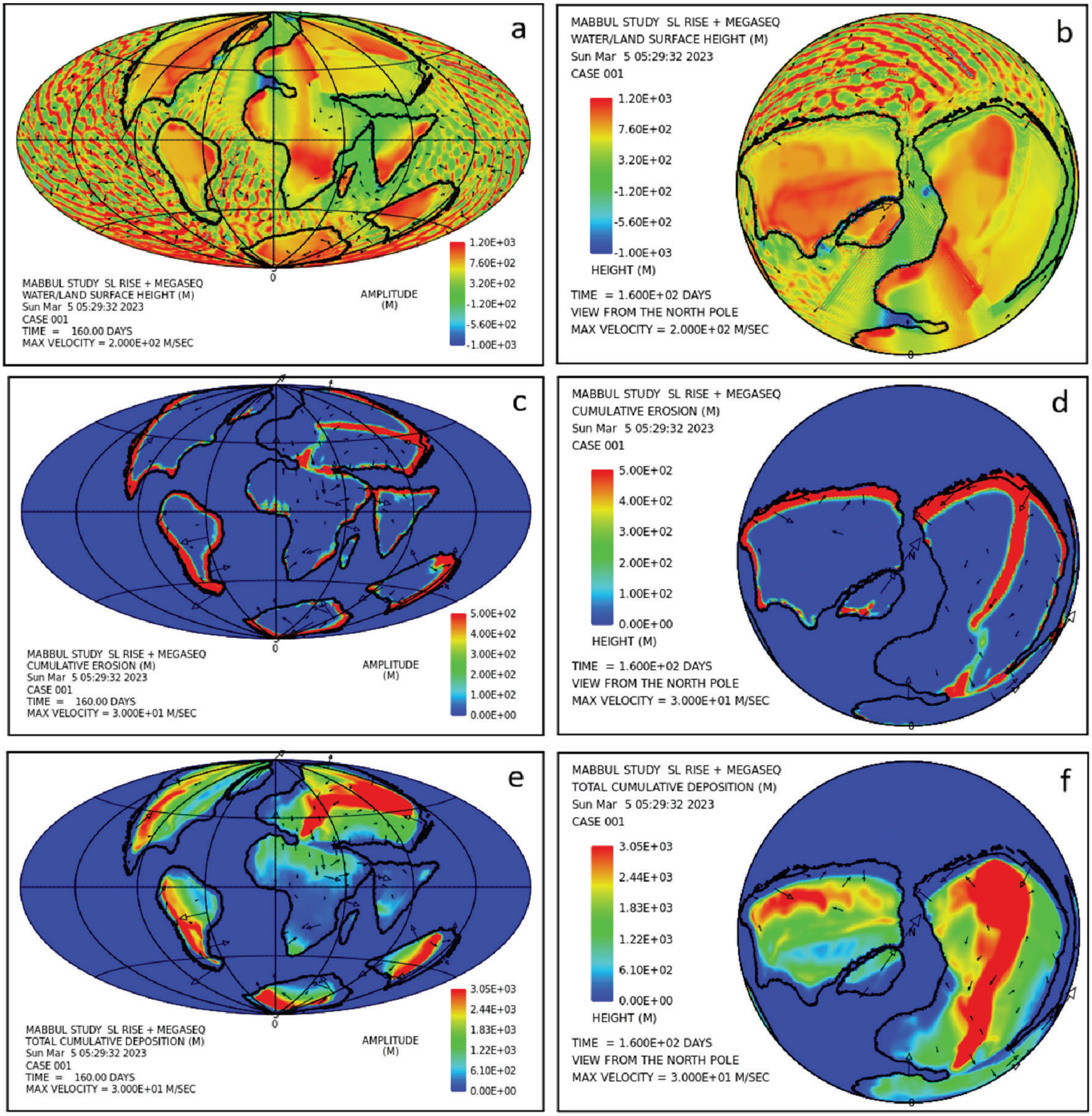

Figure 11. Plots at 160 days of water/land surface height (a), (b); cumulative depth of bedrock erosion, (c), (d); and cumulative depth of deposited sediment, (e), (f). Mean sediment depth is 1230 m.

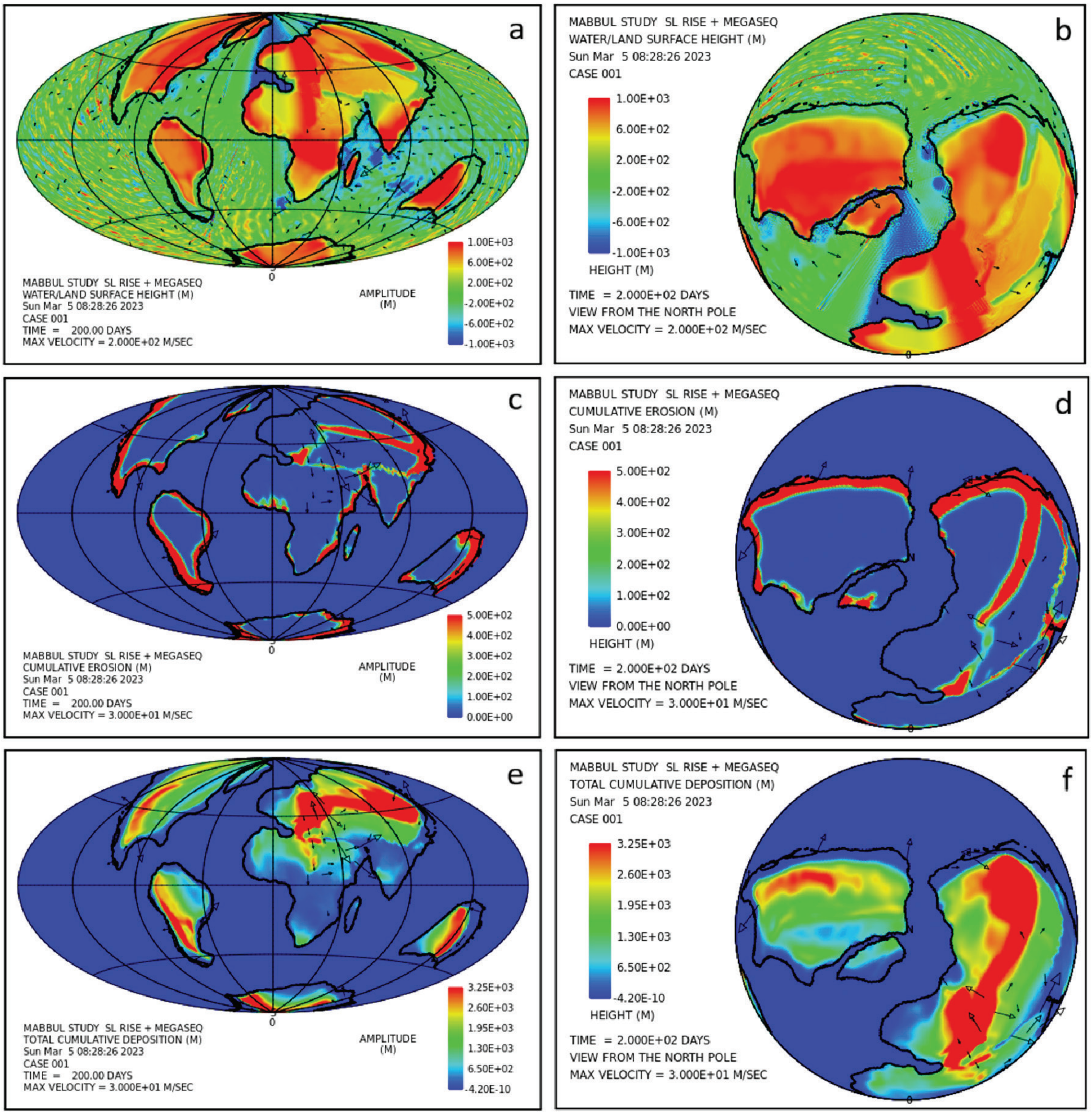

Figure 12. Plots at 200 days of water/land surface height (a), (b); cumulative depth of bedrock erosion, (c), (d); and cumulative depth of deposited sediment, (e), (f). Mean sediment depth is 1489 m.

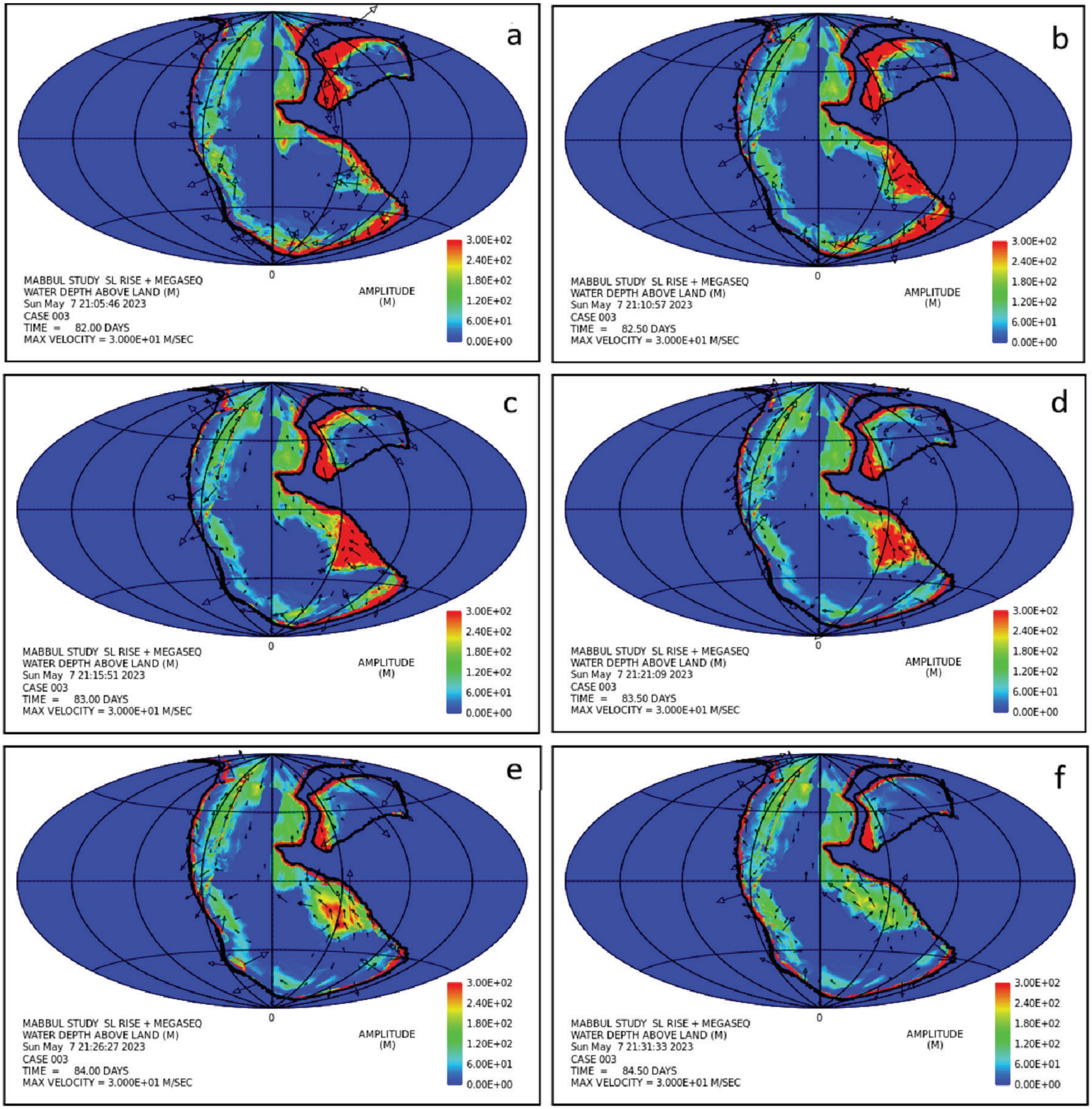

Figure 13. Water height above the land surface, denoted by color, and water velocities, denoted by arrows. For visualization purposes, water heights are clipped at 300 m, and water velocities are clipped at 30 m/s. Snapshots are spaced 12 hours apart beginning at 82 days. Note the large water pulse that invades the continental surface below the equator between 45° and 90° longitude and then drains away.

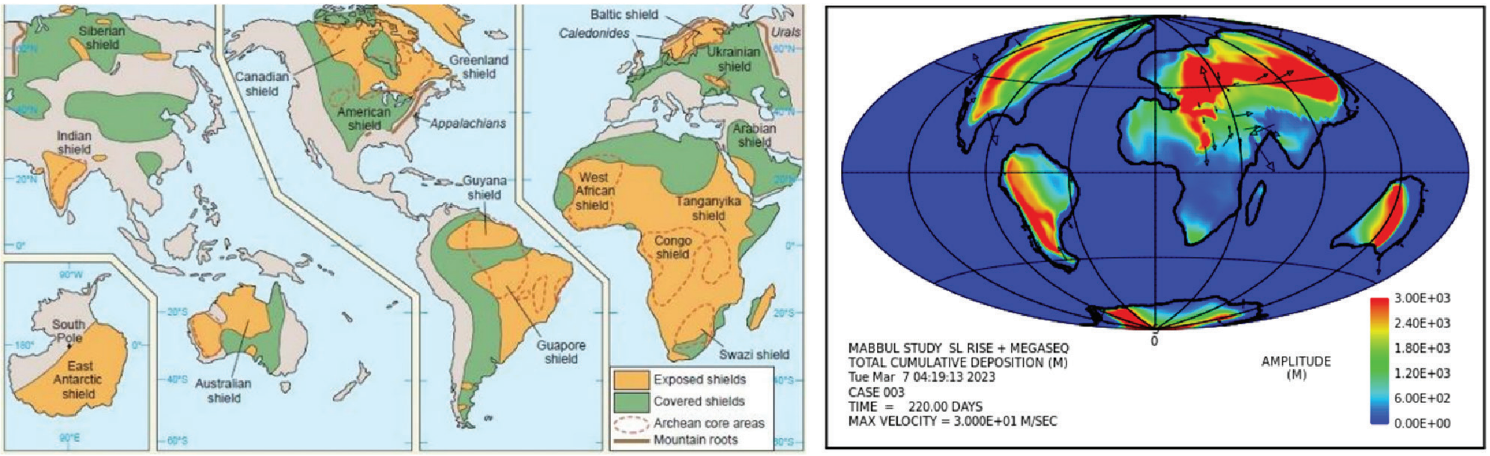

Figure 14. Comparison of the observed distribution of continental sediment on earth today (left) and the distribution of sediment obtained in the illustrative calculation at a time of 220 days (right). The gray regions in the left panel are recent tectonic belts that in many cases contain substantial thicknesses of sediment. The exposed shields correspond to regions with crystalline bedrock largely barren of sediment at the surface.

deep ocean floor. Not just any mechanism would lead to the creation, transport, and deposition of such a staggering amount of sediment on the surface of the continents. In this model it is accomplished by tsunamis generated in the deep ocean basins, which then impinge violently upon the continent margins, erode those margins, and carry the resulting sediment particles far inland to be deposited in the continent interiors. Just what other candidate mechanism might achieve this?

B. Small picture details

But what about the processes at the shorter length scales? In terms of volume, fine-grained sedimentary rocks (shales, mudstones, siltstones, etc.) are the dominant sedimentary rock type, constituting some two-thirds of the sedimentary rock inventory (Potter et al. 2005). Such rocks until fairly recently were thought to have formed in low-energy conditions of offshore and deeper-water environments. However, during the past twenty years a revolution, driven largely by careful laboratory flume experiments, has occurred in understanding how these rocks form (Schieber et al. 2007; Schieber and Southard 2009; Wilson and Schieber 2014; Schieber et al. 2022). These experiments demonstrate consistently that sand-sized floccules of agglomerated clay particles deposit rapidly from bedload transport in laboratory flumes to produce plane-bedded and ripple cross-laminated bedforms. Plane-bedded mud laminae form from bedload transport at current velocity of approximately 0.5 meter per second. Ripple laminated mud deposits at velocity of 0.25 meter per second. There is now growing consensus that most mudstones in fact are dominated by bedforms formed by current deposition of flocculated clays from moving bedload. This applies to prominent North American shales such as the New Albany Shale, Genesee Group shales, (Wilson and Schieber 2014) and Mancos Shale.

This research confirmed by field observation not only demonstrates that most mudrocks deposit as sand-sized clay floccules from moving water, but the research further shows that conclusion is true for carbonate sediments as well. The abstract of a paper from ten years ago (Schieber et al. 2013) states this clearly:

> Flume experiments with fine-grained carbonate particles (< 62.5 mm) show that they form floccules that travel in bedload, form current ripples, and deposit laminated sediments. In order to compare our flume experiments to work on sand transport, we ran flume experiments with medium sand and observed that the velocities at which sand grains started to move and form ripples were in the same range as those where floccules move and form ripples. These ripples are in essence identical to those formed by clay-mineral floccules or sand grains under similar conditions. In light of previous experiments with clay minerals, these results indicate that, of the key controls on mud deposition, flocculation and suspended-sediment concentration are more important than particle mineralogy or water chemistry, and are about as important as bottom shear stress for deposition.
>
> Suspensions of carbonate mud show the same pattern of flocculation, ripple formation, and bed accretion as observed previously in experiments with clay-mineral suspensions. The resulting carbonate mud deposits show internal low-angle (2–5 degrees) laminae, and in plan view a pattern of ripple foresets that is identical to rib-and-furrow structure in sandstones.
>
> Just as previously assumed for terrigenous muds, there has been a long-standing notion that accumulation of abundant carbonate mud reflects quiescent conditions of offshore and deeper-water environments. These experiments demonstrate unequivocally that carbonate muds can also accumulate in energetic settings. In the sedimentary record of carbonate rocks, interbedded grainstones and lime mudstones may thus not necessarily reflect shifts in depositional energy (or water depth), but alternatively may imply a shift in supplied sediment type. The observations we report suggest that published interpretations of ancient lime muds and derived paleoceanographic conditions may need to be reevaluated.

The turbulent transport submodel in MABBUL already includes most of the features required to represent mud deposition and mudrock formation as well as equivalent processes for carbonate rocks.

Specifically, it already treats an arbitrary number of sediment particle size classes, an arbitrary distribution of sediment fractions among those size classes, and an arbitrary number of vertical sublayers of user-defined thicknesses in the water column above the continent. Therefore, detailed treatment of bedload is already an available feature. Currently, the number of sediment classes is chosen to be three, with particle sizes of 0.063 mm, 0.25 mm, and 1.0 mm, and class fractions of 0.70, 0.20, and 0.10. Currently, there are eight layers in the water column, with the thickness of the bottommost layer of 1 cm. With these default choices, MABBUL's current treatment of the 0.063 mm fine sand particles should be doing a respectable proxy job of representing behavior of flocculating clay and carbonate particles. A desirable future enhancement certainly would be to include suitable diagnostics to track and output formation of these rock species, including predicted the bedforms. Even so, MABBUL already accounts for these main aspects of turbulent transport and deposition of sediment particles at the small spatial scales.

C. Megasequences—A new causal explanation

As previously discussed, the fossil-bearing sediment record displays a structure consisting of six massive sediment layer packages known as megasequences separated from one another by global-scale erosional unconformities. This paper offers an explanation for this striking feature. The explanation relates to a crucial aspect of the CPT framework, namely, the imperative of rapid and extraordinary cooling of the newly forming ocean plates. The reason is that all the pre-Flood seafloor gets recycled into the mantle well before the continents reach their current locations. Without extra cooling of the newly forming ocean lithosphere, the runaway process would cease, and CPT would come to an abrupt halt. Since the first paper on CPT (Baumgardner 1986) it has been assumed that the enhanced cooling of the new oceanic lithosphere occurred at a steady and uniform rate. However, as discussed earlier, having this cooling instead occur in discrete episodes yields abrupt drops in global sea level and provides a simple means for explaining the erosional unconformities that bound the megasequences above and below.

From its beginning the CPT framework already included one such episode to account for the runoff of water from the continents at the close of the Flood. The new approach includes six additional episodes. In quantitative terms, the amount of new ocean lithosphere generated by rapid seafloor spreading during the Flood, apart from any enhanced cooling, would produce some 5,400 m of cumulative sea bottom rise. The new approach assumes an episode of cooling sufficient to cause a 700 m drop in average sea bottom height and produce the erosional unconformity observed at the base of each of the six megasequences for a total of 4,200 m of cumulative sea bottom drop. A final episode of cooling at the top of the sixth megasequence results in an additional 1,200 m of sea bottom drop, corresponding to the runoff phase of the Flood. This final sea bottom drop therefore restores the global sea level to what it was before the onset of the cataclysm.

Note that this final cooling episode brought the temperature profile of oceanic lithosphere quickly to what we observe it to be presently. The resulting drop in global sea level allowed the water that had covered the continent surfaces to drain rapidly back into the deepened ocean basins, which moved significant quantities of sediment from continent interiors to the continental shelves. Notably, this episode of lithospheric cooling also caused the earth's outer shell of rock to become dramatically more rigid and less deformable. This, in turn, caused plate speeds to plummet and CPT to end.

Before such abrupt sea bottom drops were incorporated into the MABBUL framework, the authors were uncertain whether the numerics would remain stable. We were pleased to find that MABBUL could accommodate 700 m drops in the mean sea bottom height, each during a time span of 24 hours, with no discernable negative consequences. As expected, a significant fraction of the water that had been on the continent surfaces drains back into the ocean following each episode of sea bottom drop.

As of yet MABBUL does not have diagnostics to characterize the sedimentary signature of these episodes of dramatic sea level drop in a satisfactory manner. In the rock record a notable feature associated with some of the megasequence boundaries are extensive sandstone sheets just above those boundaries. Examples include the Tapeats Sandstone at the base of the Sauk megasequence and the St. Peter Sandstone at the base of the Tippecanoe megasequence. What MABBUL with its present diagnostics does show clearly, however, is that as the tsunami-driven pulses of sediment-laden water move inland, there is a progression in particle size deposition, with coarsest particles falling from suspension first and depositing closest to the coast and finer particles remaining in suspension longer and depositing further inland. Just how that sediment distribution is modified in MABBUL in response to an abrupt sea level drop followed by a steady sea level rise accompanied by repetitive tsunamis is a topic for future study. To the authors it will not be surprising if the result is a laterally extensive sandstone sheet extending inland from the continent margin.

D. New possible trigger for runaway subduction

A longstanding enigma in the framework of catastrophic plate tectonics has been what initiated the peeling away of oceanic lithosphere at the earth's surface and its sinking into the mantle in a runaway manner? The proposal that the cause for the erosional discontinuities that form the megasequence boundaries was sudden and extraordinary cooling of oceanic lithosphere resulting in an abrupt drop in global sea level logically brings with it a possible mechanism for the initiation the CPT cataclysm itself. In very brief terms, such an abrupt cooling of the rock layer beneath the ocean bottom increases its density appreciably and also makes it significantly more unstable to runaway sinking into the mantle below. Not only does the proposed cooling episode at the base of the Sauk megasequence appear to account for the spectacular megabreccia deposits along the western margin of North America (Sigler and Van Wingerden 1998; Van Wingerden 2003) and other evidences of extreme catastrophism at the stratigraphic discontinuity known as the Great Unconformity, it also provides a simple and yet plausible triggering mechanism for the runaway motions within the mantle that drive the entire ensuing cataclysm. This proposed trigger relies on no intermediate mechanisms or hypotheses but instead upon God's direct supernatural intervention.

VI. CONCLUSION

Numerical simulation offers a means for investigating phenomena that are impossible, either because of their physical scale or the extreme conditions they entail, or both, to explore experimentally in a repeatable manner in the laboratory. The Genesis Flood certainly falls into this category. This paper describes a beginning attempt to apply known physical laws, physical processes that can be investigated in the laboratory, and processes on larger scales that can be studied and characterized by measurements in the present, to model important aspects of this unique cataclysmic event. The numerical model exploits the shallow water approximation to represent water flow in a thin layer on the surface of a rotating sphere corresponding to the earth. It utilizes the theory of open-channel flow to treat the suspension and transport of sediment by turbulent flowing water. As its mechanism for erosion, it utilizes cavitation. To drive the water flow it draws upon a currently observable consequence of plate tectonics, namely, the locking and sudden release of the overriding lithospheric plate along its fault contact with a subducting plate in a subduction zone. Today, when the overriding plate unlocks and rebounds, its upward motion can, and often does, generate a water wave known as a tsunami. During the Flood, when plate speeds were orders of magnitude higher than they are today, the amplitudes of the tsunamis were almost certainly vastly larger.

In our numerical model we utilize such large-amplitude tsunamis to drive the global water flow. Along the continental margins water speeds consistently exceed the cavitation threshold, leading to intense erosion of the continental bedrock. As the tsunamis surge onto the continental surface, the turbulent water transports the eroded sediment inland and deposits it in patterns characterized by large spatial scales. In the case highlighted in this paper, erosion and deposition rates approach those needed to account for the average sediment thickness on today's continental surface.

This numerical model sheds important light on major issues related to the Flood. It plausibly points to the source of a large fraction of sediment in the continental sediment record within the Biblical time span of the Flood. It plausibly explains how this sediment came to be deposited on top of the normally high-standing continental surface. It readily accounts for the vast lateral scales and the horizontal continuity of these sedimentary sequences. Astonishingly, it yields a large-scale pattern of sediment distribution that matches the observed pattern remarkably well. Moreover, it suggests a plausible cause for the global erosional unconformities bounding the megasequences above and below, including the Great Unconformity. Finally, it offers a new candidate mechanism for triggering the runaway instability associated with catastrophic plate tectonics.

REFERENCES

Armitage, M. and K.L. Anderson. 2013. Soft sheets of fibrillar bone from a fossil of the supraorbital horn of the dinosaur Triceratops horridus. *Acta Histochemica* 115(6):603-608. DOI: 1016/j.acthis.2013.01.001.

Austin, S.A. (editor) 1994. *Grand Canyon: Monument to Catastrophe.* Santee, CA: Institute for Creation Research.

Baumgardner, J.R. 1986. Numerical simulation of the large-scale tectonic changes accompanying the Flood. In R. E. Walsh, C.L. Brooks, and R.S. Crowell (editors), *Proceedings of the International Conference on Creationism*, vol. 1:II, pp. 17-30. Pittsburgh, PA: Creation Science Fellowship, Inc.

Baumgardner, J.R. 1990. 3-D finite element simulation of the global tectonic changes accompanying Noah's Flood. In R. E. Walsh and C. L. Brooks (editors), *Proceedings of the Second International Conference on Creationism*, vol. 2:II, pp. 35-46. Pittsburgh, PA: Creation Science Fellowship, Inc.

Baumgardner, J. R. 1994. Computer modeling of the large-scale tectonics associated with the Genesis Flood. In R. E. Walsh (editor), *Proceedings of the Third International Conference on Creationism*, Technical Symposium Sessions, pp. 49-62. Pittsburgh, Pennsylvania: Creation Science Fellowship.

Baumgardner, J. R. 2003. Catastrophic plate tectonics: the physics behind the Genesis Flood. In R. L. Ivey, Jr. (editor), *Proceedings of the Fifth International Conference on Creationism*, pp. 113–126. Pittsburgh, Pennsylvania: Creation Science Fellowship.

Baumgardner, J.R. 2013. Explaining the continental fossil-bearing sediment record in terms of the Genesis Flood: Insights from numerical modeling of erosion, sediment transport, and deposition processes on a global scale. In M. Horstemeyer (editor), *Proceedings of the Seventh International Conference on Creationism*, article 3. Pittsburgh, Pennsylvania: Creation Science Fellowship, Inc.

Baumgardner, J. 2018a. Numerical modeling of the large-scale erosion, sediment transport, and deposition processes of the Genesis Flood. *Answers Research Journal* 11:149–170.

Baumgardner, J. 2018b. Understanding how the Flood sediment record was formed: The role of large tsunamis. In J. H. Whitmore (editor), *Proceedings of the Eighth International Conference on Creationism*, pp. 287–305. Pittsburgh, Pennsylvania: Creation Science Fellowship.

Bird, P. 2003. An updated digital model of plate boundaries. *Geochemistry Geophysics Geosystems* 4(3), 1027, doi:10.1029/2001GC000252.

Blakey, R.C. 2008. Gondwana paleogeography from assembly to breakup—A 500 m.y. odyssey. In *Resolving the Late Paleozoic Ice Age in Time and Space*, Special Paper 441, C.R. Fielding, T.D. Frank, and J.L. Isbell (editors), pp. 1-28. Boulder, CO: The Geological Society of America. DOI: 10.1130/2008.2441(01).

Clarey, T.L. and D.J. Werner. 2017. The sedimentary record demonstrates minimal flooding of the continents during Sauk deposition. *Answers Research Journal* 10:271–283.

Clarey, T. 2020. *Carved in Stone*. Dallas: Institute for Creation Research.

Heap, A.D. and P.T. Harris, 2008. Geomorphology of the Australian margin and adjacent seafloor. *Australian Journal of Earth Sciences* 55:555-585.

Lindberg, F.A. (editor) 1986. *Correlation of Stratigraphic Units of North America* (COSUNA): Correlation Chart Series. Tulsa, Oklahoma: American Association of Petroleum Geologists.

Majewski, D., D. Liermann, P. Prohl, B. Ritter, M. Buchhold, T. Hanisch, G. Paul, W. Wergen, and J. Baumgardner. 2002. The operational global icosahedral-hexagonal grid point model GME: Description and high resolution tests. *Monthly Weather Review* 130:319–338.

Nanson, R., A. Carroll, Z. Huang, S. Nichol, and K. Miller. 2018. An eco-narrative of Gifford Marine Park: Temperate East marine region. *Report to the National Environmental Science Programme, Marine Biodiversity Hub*. Geoscience Australia.

Olson, P., E. Reynolds, L. Hinnov, and A. Goswami. 2016. Variation of ocean sediment thickness with crustal age. *Geochemistry, Geophysics, Geosystems* 17(4):1349-1369.

Plet, C., K. Grice, A. Pagès, M. Verrall, M.J.L. Coolen, W. Ruebsam, W.D.A. Rickard, and L. Schwark. 2017. Palaeobiology of red and white blood cell-like structures, collagen and cholesterol in an ichthyosaur bone. *Scientific Reports* 7(13776)1-10. DOI: 10.1038/s41598-017-13873-4.

Potter, P.E., J.B. Maynard, and P,J. Depetris. 2005. *Mud and Mudstones:*

Introduction and Overview. New York: Springer. DOI: 10.1007/b138571.

Prawirodirdjo, L., and Bock, Y. (2004). Instantaneous global plate motion model from 12 years of continuous GPS observations. *Journal of Geophysical Research: Solid Earth*, 109(B8).

Prothero, D.R., and F. Schwab. 2004. *Sedimentary geology: An introduction to sedimentary rocks and stratigraphy,* 2nd Edition, pp. 12–14. New York: W.H. Freeman.

Richardson, L.F. 1920. The supply of energy from and to atmospheric eddies. *Proceedings of the Royal Society of London*, Series A, 97, no. 686:354–37.

Schieber, J., J.B. Southard, and K. Thaisen. 2007. Accretion of mudstone beds from migrating floccule ripples. *Science* 318:1760–1763. DOI: 10.1126/science.1147001.

Schieber, J. and J.B. Southard. 2009. Bedload transport by floccule ripples—Direct observation of ripple migration processes and their implications. *Geology* 37:483-486. DOI: 10.1130/G25319A.1.

Schieber, J., J.B. Southard, P. Kissling, B. Rossman, and R. Ginsburg. 2013. Experimental deposition of carbonate mud from moving suspensions: Importance of flocculation and implications for modern and ancient carbonate mud deposition. *Journal of Sedimentary Research* 83:1025-1031. DOI: 10.2110/jsr.2013.77.

Schieber, J., Z. Li, Z. Yawar, X. Cao, T. Ashley, and R. Wilson. 2022. Kaolinite deposition from moving suspensions: The role of flocculation, salinity, suspended sediment concentration and flow velocity/bed shear. *Sedimentology* 70:121-144. DOI: 10.1111/sed.13034.

Schweitzer, M.H., Wittmeyer, J.L., Horner, J.R., and J. K. Toporski. 2005. Soft-tissue vessels and cellular preservation in Tyrannosaurus rex. *Science* 307(5717):1952–1955. DOI: 10.1126/science.1108397.

Scotese, C.R. 2021. An atlas of phanerozoic paleogeographic maps: The seas come in and the seas go out. *Annual Review of Earth and Planetary Sciences* 49:679-728. DOI: 10.1146/annurev-earth-081320-064052.

Sigler, R. and C. Van Wingerden 1998. Submarine flow and slide deposits in the Kingston Peak Formation, Kingston Range, Mojave Desert, CA: Evidence for catastrophic initiation of Noah's Flood. In R.E. Walsh (editor), *Proceedings of the Fourth International Conference on Creationism*, pp. 487-502. Pittsburgh, Pennsylvania: Creation Science Fellowship.

Sloss, L.L. 1963. Sequences in the cratonic interior of North America. *Geological Society of America Bulletin* 74:93–114.

Solomon, S.C. and D.R. Toomey. 1992. The structure of mid-ocean ridges. *Annual Reviews of Earth and Planetary Science* 20:329-264

Staniforth, A. and J. Cote. 1991. Semi-Lagrangian integration schemes for atmospheric models—a review. *Monthly Weather Review* 119:2206–2223.

Van Wingerden, C. 2003. Initial Flood deposits of the western North American cordillera: California, Utah and Idaho, In R. L. Ivey, Jr. (editor), *Proceedings of the Fifth International Conference on Creationism*, pp. 349-358. Pittsburgh, Pennsylvania: Creation Science Fellowship.

Vreugdenhil, C.B. 1994. *Numerical Methods for Shallow Water Flow*. Boston: Kluwer Academic Publishers

Wilson, R.D. and Schieber, J. 2014. Muddy prodeltaic hyperpycnites in the lower Genesee Group of central New York, USA: Implications for mud transport in epicontinental seas. *Journal of Sedimentary Research* 84:866-874. DOI: 10.2110/jsr.2014.70.

Winston, D., and P.K. Link. 1993. Middle Proterozoic rocks of Montana, Idaho, and Washington: The Belt Supergroup. In J. Reed, P. Simms, R. Houston, D. Rankin, P. Link, R. Van Schmus, and P. Bickford (editors), *Precambrian of the conterminous United States*, pp. 487–521. Boulder, Colorado: Geological Society of America, The Geology of North America, v. C-3.

THE AUTHORS

John Baumgardner has a Ph.D. in geophysics from UCLA and worked in computational physics at Los Alamos National Laboratory for most of his scientific career. Since the 1980's he has published extensively on catastrophic plate tectonics and the Genesis Flood. He served on the Radioisotopes and the Age of the Earth (RATE) team that documented multiple lines of radioisotope evidence that the earth is young. More recently he has developed software to study the transport and deposition of sediment produced by giant tsunamis during the Flood. He currently is research professor emeritus in the School of Engineering at Liberty University.

Evan Navarro has a B.S. in mechanical engineering from the University of Virginia, with a concentration in materials science. For the past five years he has worked as a design engineer for Delta Star, Inc., in the realm of mobile high voltage transformers. He has a strong desire to honor God by applying his talents and training to issues in creation apologetics, especially to the reality of the Genesis Flood.